

AD-A091 230

DAYTON UNIV OH RESEARCH INST

F/G 11/6

SURFACE CHARACTERIZATION OF CHEMICALLY ETCHED TI-8AL-1MO-15N AN--ETC(U)

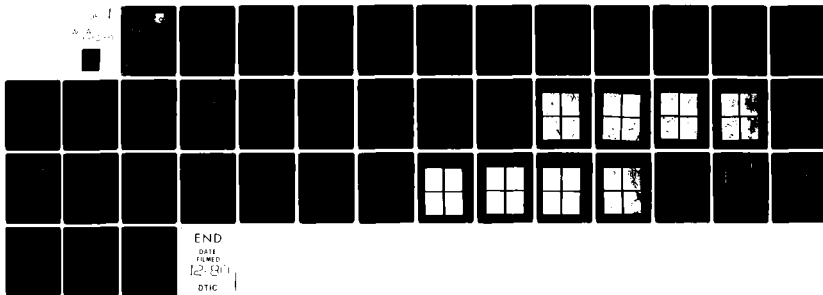
AUG 80 J S SOLOMON, A A ROCHE, W L BAUM

F33615-78-C-5102

UNCLASSIFIED

AFWAL-TR-80-8105

NL



18
19
AFWAL TR-80-4105



LEVEL

AD A 091230

6
SURFACE CHARACTERIZATION OF
CHEMICALLY ETCHED
Ti-8Al-1Mo-1Sn and Ti-13V-11Cr-3Al

10 I. S. SOLOMON A. A. Roche W. L. Baun

UNIVERSITY OF DAYTON RESEARCH INSTITUTE
DAYTON, OHIO 45469

15 FB 9615-78-C-5102

A. A. ROCHE
UNIVERSAL ENERGY SYSTEMS
DAYTON, OHIO 45432

NOT RECORDED
NOV 3 1980

W. L. BAUN
MECHANICS AND SURFACE INTERACTIONS BRANCH
NONMETALLIC MATERIALS DIVISION

16 2429

11 AUGUST 1980

12 73

TECHNICAL REPORT AFWAL TR 80-4105
9 Final Report for Period June 1979 to February 1980

17 02

DDC FILE COPY

Approved for public release; distribution unlimited.

MATERIALS LABORATORY
AIR FORCE WRIGHT AERONAUTICAL LABORATORIES
AIR FORCE SYSTEMS COMMAND
WRIGHT-PATTERSON AIR FORCE BASE, OHIO 45433

105 400


80 10 31 179

NOTICE

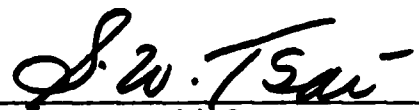
When Government drawings, specifications, or other data are used for any purpose other than in connection with a definitely related Government procurement operation, the United States Government thereby incurs no responsibility nor any obligation whatsoever; and the fact that the Government may have formulated, furnished, or in any way supplied the said drawings, specifications, or other data, is not to be regarded by implication or otherwise as in any manner licensing the holder or any other person or corporation, or conveying any rights or permission to manufacture, use, or sell any patented invention that may in any way be related thereto.

This report has been reviewed by the Office of Public Affairs (ASD/PA) and is releasable to the National Technical Information Service (NTIS). At NTIS, it will be available to the general public, including foreign nations.

This technical report has been reviewed and is approved for publication.

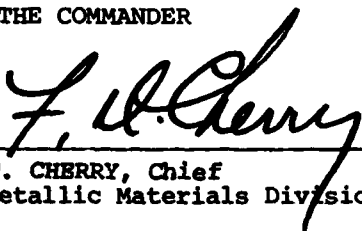


W. L. Baun, Project Engineer
Mechanics & Surface Interactions Br.
Nonmetallic Materials Division



S. W. TSAI, Chief
Mechanics & Surface Interactions Br.
Nonmetallic Materials Division

FOR THE COMMANDER



F. D. CHERRY, Chief
Nonmetallic Materials Division

"If your address has changed, if you wish to be removed from our mailing list, or if the addressee is no longer employed by your organization please notify AFWAL/MLEM, WPAFB, OH 45433 to help us maintain a current mailing list."

Copies of this report should not be returned unless return is required by security considerations, contractual obligations, or notice on a specific document.

UNCLASSIFIED

SECURITY CLASSIFICATION OF THIS PAGE (When Data Entered)

REPORT DOCUMENTATION PAGE		READ INSTRUCTIONS BEFORE COMPLETING FORM
1. REPORT NUMBER AFWAL-TR-80-4105 ✓	2. GOVT ACCESSION NO. AD-A091 230	3. RECIPIENT'S CATALOG NUMBER
4. TITLE (and Subtitle) SURFACE CHARACTERIZATION OF CHEMICALLY ETCHED Ti-8Al-1Mo-1Sn AND Ti-13V-11Cr-3Al ✓		5. TYPE OF REPORT & PERIOD COVERED Internal June 1979 to February 1980
		6. PERFORMING ORG. REPORT NUMBER
7. AUTHOR(s) J. S. Solomon, A. A. Roche, and W. L. Baun		8. CONTRACT OR GRANT NUMBER(s) Inhouse, AF33615-78-C-5102 and AF33615- - -5129 ✓
9. PERFORMING ORGANIZATION NAME AND ADDRESS Materials Laboratory Air Force Wright Aeronautical Laboratories, AFSC Wright-Patterson AFB, Ohio 45433 ✓		10. PROGRAM ELEMENT, PROJECT, TASK AREA & WORK UNIT NUMBERS Project 2419, Task 241902, WU #44
11. CONTROLLING OFFICE NAME AND ADDRESS Materials Laboratory (AFWAL/MLBM) Air Force Wright Aeronautical Laboratories, AFSC Wright-Patterson AFB, Ohio 45433		12. REPORT DATE August 1980 ✓
		13. NUMBER OF PAGES 43
14. MONITORING AGENCY NAME & ADDRESS (if different from Controlling Office)		15. SECURITY CLASS. (of this report) Unclassified
		15a. DECLASSIFICATION/DOWNGRADING SCHEDULE
16. DISTRIBUTION STATEMENT (of this Report) Approved for public release; distribution unlimited.		
17. DISTRIBUTION STATEMENT (of the abstract entered in Block 20, if different from Report)		
18. SUPPLEMENTARY NOTES		
19. KEY WORDS (Continue on reverse side if necessary and identify by block number) Titanium Alloy, Surface Treatment, Surface Characterization, Secondary Ion Mass Spectroscopy, Auger Electron Spectroscopy, Ion Scattering Spectroscopy, Scanning Electron Microscopy		
20. ABSTRACT (Continue on reverse side if necessary and identify by block number) The effects of chemical treatments on surfaces of Ti-8Al-1Mo-1Sn and Ti-13V-11Cr-3Al were characterized with Auger electron spectroscopy, ion scattering spectroscopy, secondary ion mass spectroscopy, and scanning electron microscopy. The effects of particular treatments were not always the same for each alloy. In all cases the original surface oxide was replaced with a new one containing traces of elemental species common to a particular treatment. In most cases the oxide formed was identified as TiO ₂ . The oxide formed on Ti-8Al-1Mo-1Sn by a fluorophosphate treatment was an oxyfluoride of titanium. ←		

FOREWORD

This technical report was prepared by J. S. Solomon of the University of Dayton Research Institute, Dayton, Ohio, A. A. Roche of Universal Energy Systems, Dayton, Ohio, and W. L. Baun of the Mechanics and Surface Interactions Branch, Nonmetallic Materials Division, Air Force Wright Aeronautical Laboratories, Wright-Patterson Air Force Base, Ohio. The work was initiated under Project 2419 "Nonmetallic and Composite Materials", and was administered by the Air Force Wright Aeronautical Laboratories, Air Force Systems Command, Wright-Patterson Air Force Base, Ohio.

This work covers work conducted inhouse during the period June 1979 to February 1980.

Accession For	
NTIS GRAB	<input checked="" type="checkbox"/>
DTIC TAB	<input type="checkbox"/>
Unannounced	<input type="checkbox"/>
Justification	<input type="checkbox"/>
By _____	
Distribution/	
Availability Codes	
Avail and/or	
Dist _____	
A	

TABLE OF CONTENTS

Section		Page
I	INTRODUCTION	1
II	EXPERIMENTAL	1
III	RESULTS	4
	A. Ti-8Al-1Mo-1Sn	4
	B. Ti-13V-11Cr-3Al	13
IV	DISCUSSION	25
V	CONCLUSIONS	30
	REFERENCES	35

LIST OF ILLUSTRATIONS

Figure		Page
1	AES Spectra of "As Received" Ti-8Al-1Mo-1Sn	5
2	ISS Spectra of "As Received" Ti-8Al-1Mo-1Sn (a) First Trace and (b) Second Trace	6
3	He ⁺ SIMS Spectrum of "As Received" Ti-8Al-1Mo-1Sn	7
4	AES Spectra of ES Ti-8Al-1Mo-1Sn	8
5	Ar ⁺ SIMS Spectrum of ES Ti-8Al-1Mo-1Sn	9
6	AES Spectra of (a) Argon Sputtered ES and (b) Xenon Sputtered ES Surfaces of Ti-8Al-1Mo-1Sn	10
7	SEM Micrographs of Ti-8Al-1Mo-1Sn Subjected to Treatments 1 (B ₁) and 2 (B ₁₋₂)	14
8	SEM Micrographs of Ti-8Al-1Mo-1Sn Subjected to Treatments 3 (B ₁₋₃) and 4 (B ₁₋₄)	15
9	SEM Micrographs of Ti-8Al-1Mo-1Sn Subjected to Treatments 5 (B ₁₋₅) and 6 (B ₁₋₆)	16
10	SEM Micrographs of Ti-8Al-1Mo-1Sn Subjected to Treatments 7 (B ₁₋₇) and 8 (B ₁₋₈)	17
11	AES Spectra of "As Received" Ti-13V-11Cr-3Al	18
12	He ⁺ SIMS Spectrum of "As Received" Ti-13V-11Cr-3Al	19
13	AES Spectra of ES Ti-13V-11Cr-3Al	20
14	Ar ⁺ SIMS Spectrum of ES Ti-13V-11Cr-3Al	21
15	SEM Micrographs of Ti-13V-11Cr-3Al Subjected to Treatments 1 (G ₁) and 2 (G ₁₋₂)	26
16	SEM Micrographs of Ti-13V-11Cr-3Al Subjected to Treatments 3 (G ₁₋₃) and 4 (G ₁₋₄)	27
17	SEM Micrographs of Ti-13V-11Cr-3Al Subjected to Treatments 5 (G ₁₋₅) and 6 (G ₁₋₆)	28
18	SEM Micrographs of Ti-13V-11Cr-3Al Subjected to Treatments 7 (G ₁₋₇) and 8 (G ₁₋₈)	29

LIST OF ILLUSTRATIONS (Concluded)

Figure		Page
19	He ⁺ SIMS Spectrum of Ti-8Al-1Mo-1Sn Subjected to Treatment 4	31
20	AES Spectra of Ti-8Al-1Mo-1Sn Subjected to Treatment 4	32
21	He ⁺ SIMS Spectrum of Ti-13V-11Cr-3Al Subjected to Treatment 4	33
22	AES Spectra of Ti-13V-11Cr-3Al Subjected to Treatment 4	34

LIST OF TABLES

Table		Page
1	Surface Chemical Treatments for Titanium and Titanium Alloys	2
2	AES Elemental I.D. of Treated Ti-8Al-1Mo-1Sn	11
3	SIMS Elemental I.D. of Treated Ti-8Al-1Mo-1Sn	12
4	AES Elemental I.D. of Treated Ti-13V-11Cr-3Al	22
5	SIMS Elemental I.D. of Treated Ti-13V-11Cr-3Al	23
6	Oxide Thickness in Nanometers Determined by Auger Sputter Profile Analysis from Treated Ti-8Al-1Mo-1Sn and Ti-13V-11Cr-3Al	24

I. INTRODUCTION

Because of temperature and weight considerations, Ti and its alloys are used extensively by the aircraft industry. The "super" alpha Ti-8Al-1Mo-Sn alloy was developed for use in jet engines where a high fracture toughness is required. Ti-13V-11Cr-3Al has good workability and strength properties when properly heat treated. Consequently, it is easily forged and has found use in structural components.

Because of the number of alloying constituents in these alloys, there is a possibility of differences in surface versus bulk compositions, either in "as received" states or after the alloys have undergone further processing. These differences may arise from a number of processes. This may involve surface enrichment of a particular constituent with a high diffusion rate during a heat treatment. Another possibility may be either surface depletion or enrichment of one or more of the alloying elements following chemical cleaning treatments.

In this work, Ti-8Al-1Mo-1Sn and Ti-13V-11Cr surfaces were subjected to eight chemical treatments. The topological effects of the treatments were characterized with scanning electron microscopy (SEM). Changes in surface chemistry and elemental distribution were characterized with Auger electron spectroscopy (AES), ion scattering spectroscopy (ISS), and positive ion secondary ion mass spectroscopy (SIMS).

II. EXPERIMENTAL

Ti-8Al-1Mo-1Sn and Ti-13V-11Cr-3Al alloys were subjected to the chemical treatments listed in Table 1. After drying, they were analyzed with a Perkin-Elmer Physical Electronics Industries (PHI) model 540-A thin film analyzer equipped with a single pass cylindrical mirror analyzer (CMA) with a resolution $\Delta E/E \sim 0.6\%$.

TABLE 1
SURFACE CHEMICAL TREATMENTS FOR TITANIUM
AND TITANIUM ALLOYS

CODE	DESCRIPTION	TREATMENT
1	Degrease	Sample slurried in acetone, wiped dry, then ultrasonically cleaned in carbon tetrachloride for 5 minutes.
2	Alkaline	Sample submerged in 0.1N sodium hydroxide, room temperature for 2 minutes. Running tap H ₂ O for 1 minute, standing deionized H ₂ O for 5 minutes.
3	HNO ₃ /HF (fluoro-nitric)	Sample submerged in a solution of 170 ml nitric acid, 30 ml hydrofluoric acid, 800 ml distilled water, room temperature for 2 minutes. Rinse as in #2.
4	Na ₃ PO ₄ /NaF/HF (fluoro-phosphate)	Sample submerged in a solution of 50g sodium ortho phosphate, 9g sodium fluoride, 26 ml hydrofluoric acid, distilled water to 1 liter, room temperature for 2 minutes. Rinse as in #2.
5	NH ₄ HF ₂ (fluoro-ammonium)	Sample submerged in solution of ammonium bifluoride (10g/liter) room temperature for 2 minutes. Rinse as in #2.
6	H ₂ SO ₄ /CrO ₃ (sulfo-chromium)	Sample submerged in solution of 300g sulfuric acid, 40g chromium acid, distilled water to 1 liter, room temperature for 2 minutes. Rinse as in #2.
7	HNO ₃ /HF/H ₂ O ₂ /NH ₄ F, HF (fluoro-nitro-ammonium)	Sample submerged in solution of 80 ml nitric acid, 20 ml hydrofluoric acid, 20 ml hydrogen peroxide (30%), 10 ml ammonium bifluoride (saturated), distilled water 500 ml, room temperature for 2 minutes. Rinse as in #2.
8	Hot NaOH/H ₂ O ₂ (hot alkaline)	Sample submerged in solution of 20g sodium hydroxide, 20 ml hydrogen peroxide (30%), distilled water to 1 liter, 65°C temperature (150°F) for 2 minutes. Rinse as in #2.

The coaxial electron gun was operated with a 4-KeV potential at 1.0 to 5.0 μA beam current. A peak-to-peak modulation of 7 eV during broad scans (i.e., 0-2000 eV) and 2 eV for narrow scans (i.e., 330-530 eV) was applied to the analyzer for phase sensitive detection. Elemental sputter profiles were constructed using digitally recorded and computer processed N(E) data. The ion beam was generated with a PHI model 04-191 Sputter Ion Gun which was operated with a beam potential of 2 KeV and ion current density of approximately $1.9 \mu\text{A}/\text{mm}^2$ at 10 mA ion gun emission current or $0.5 \mu\text{A}/\text{mm}^2$ at 3 mA ion gun emission current.

The sputtering rate for TiO_2 under the above conditions with argon was determined to be 11.5 nanometers per minute (1 anometer (nm) = 3.94×10^{-8} in.) with an ion current density of $1.9 \mu\text{A}/\text{mm}^2$ and 2.8 nm/min with an ion current density of $0.5 \mu\text{A}/\text{mm}^2$.

Secondary ion mass spectroscopy (SIMS) analysis was performed using an EAI/1100 quadrupole mass analyzer fitted with a low resolution double-focusing ion energy filter. The same ion gun used for sputter profiling was used as the primary ion beam source for SIMS. Both He^+ and Ar^+ were used as primary ion sources. He^+ was used to obtain SIMS data from surfaces prior to sputter profiling since near static (nondestructive) conditions can be achieved with the lighter inert gas. During sputter profile analyses Ar^+ was used.

ISS data were obtained with a 3M Co. ISS instrument equipped with a cylindrical mirror analyzer and a coaxial ion gun. The analyzer acceptance angle is 137.7° . The probing beam was Ne^+ and the ion gun was operated with a potential of 1500 eV.

Pieces of the specimens for SEM analysis were coated with ~ 20 -50 nm Au in an ISI-PS-2 sputter coater. All specimens were analyzed with an ISI-60 scanning electron microscope at a tilt angle of 15° .

III. RESULTS

A. Ti-8Al-1Mo-1Sn

Figures 1-3 show the respective AES, ISS, and SIMS spectra obtained from "as received" surfaces. Figures 4 and 5 contain the respective AES and SIMS spectra from an equilibrium sputtered (ES) surface which represent the bulk. An ES surface is defined as one in which a steady-state is achieved after ion beam sputtering away surface contaminants. Figure 6 shows AES ES spectra in which the ES condition was achieved using (a) Ar and (b) Xe.

Table 2 is a semiquantitative compilation of the elements detected by AES on all the treated Ti-8Al-1Mo-1Sn surfaces. Table 3 summarizes the SIMS data from the same surfaces. All values listed in Tables 2 and 3 are normalized to Ti.

A significant difference between the different techniques is the detectability of alloying elements. In AES, the major Sn and Ti peaks overlap each other and, therefore, small amounts of either element in the presence of large amounts of the others cannot be detected with any degree of certainty. On the other hand, this problem does not occur with SIMS and as shown in Table 3, Sn was detected on the "as received" surfaces subjected to treatments 2 and 5.

Al was detected on all treated surfaces but neither AES or SIMS could be used to reliably report the presence of Mo, even after the surface oxide was removed by sputtering with argon. The problem with AES is the overlapping of the most sensitive Mo peak by the Cl and Ar peaks and relatively low sensitivity of other Mo peaks. Ar is implanted into the surface by ion beam bombardment. As shown in Figure 6 the use of Xe to sputter clean the surface does not introduce an interference with the Mo Auger peaks and Mo was detected on the ES surface. The SIMS Mo peaks are also subject to overlap by the Ti_2^+ peak and its isotopes. The detection of Mo with ISS is not subject to the peak overlap problems of the other two techniques. In addition, ISS is more

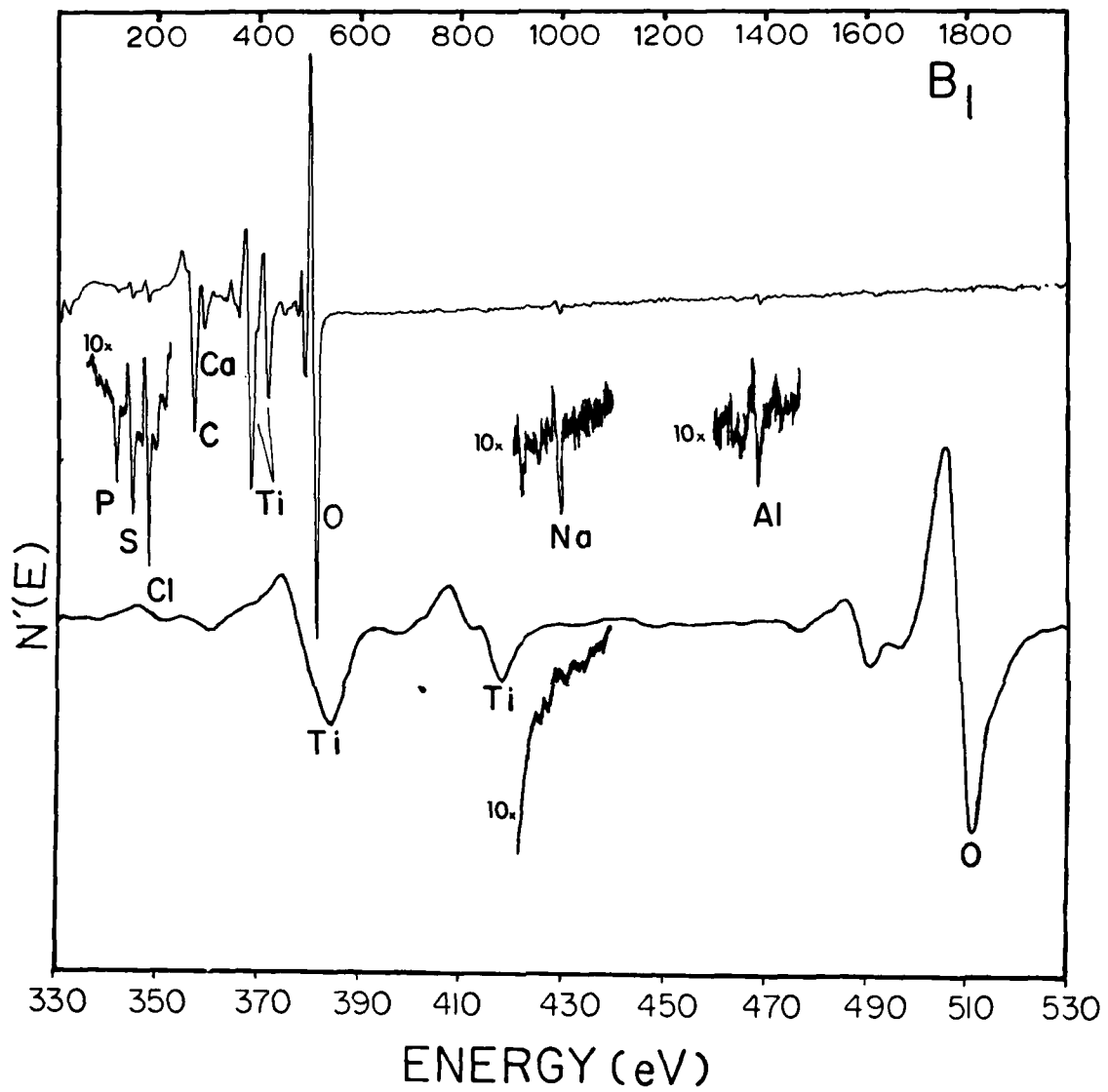


Figure 1. AES Spectra of "As Received" Ti-8Al-1Mo-1Sn.

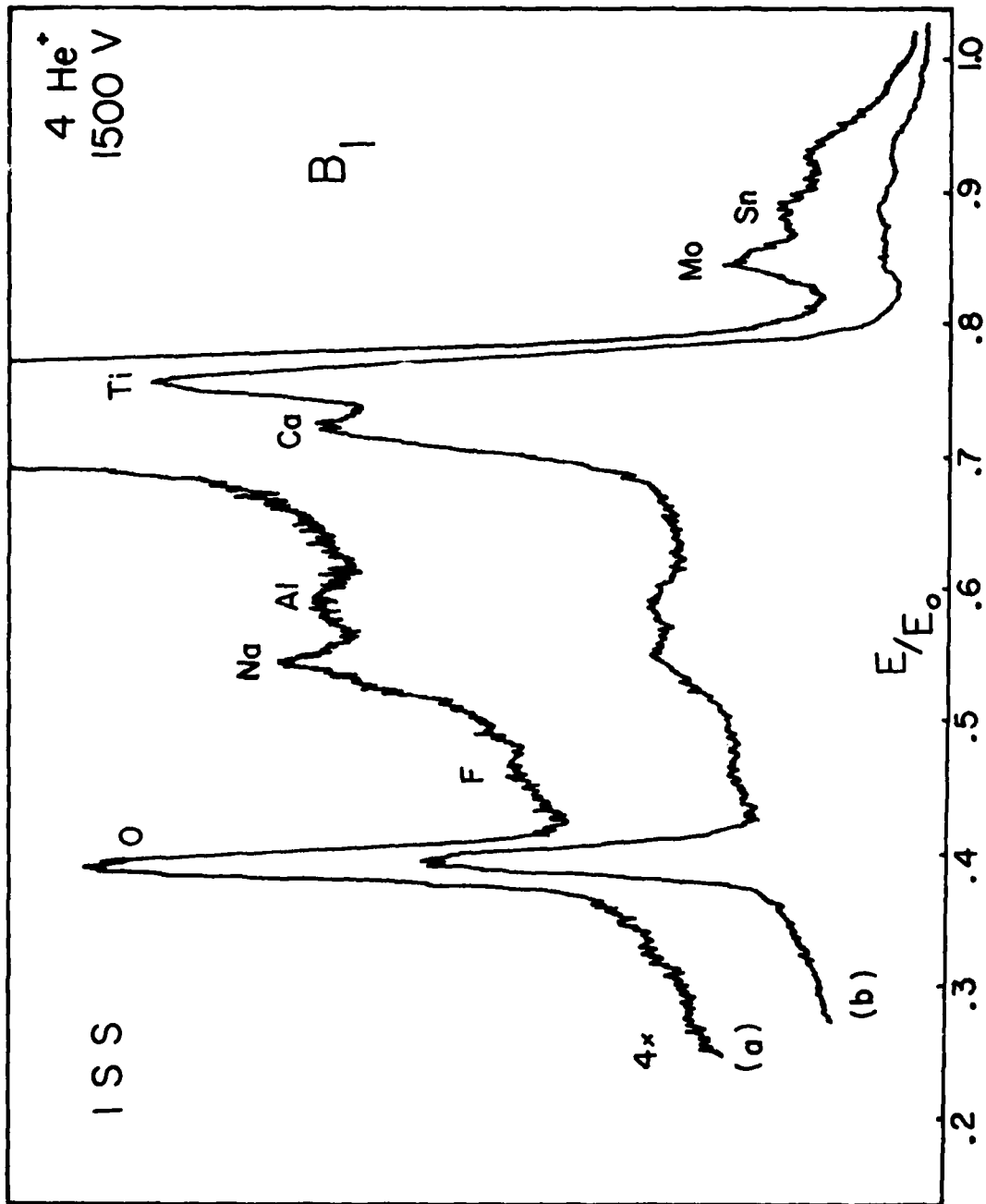


Figure 2. ISS Spectra of "As Received" Ti-8Al-1Mo-1Sn
 (a) First Trace and (b) Second Trace.

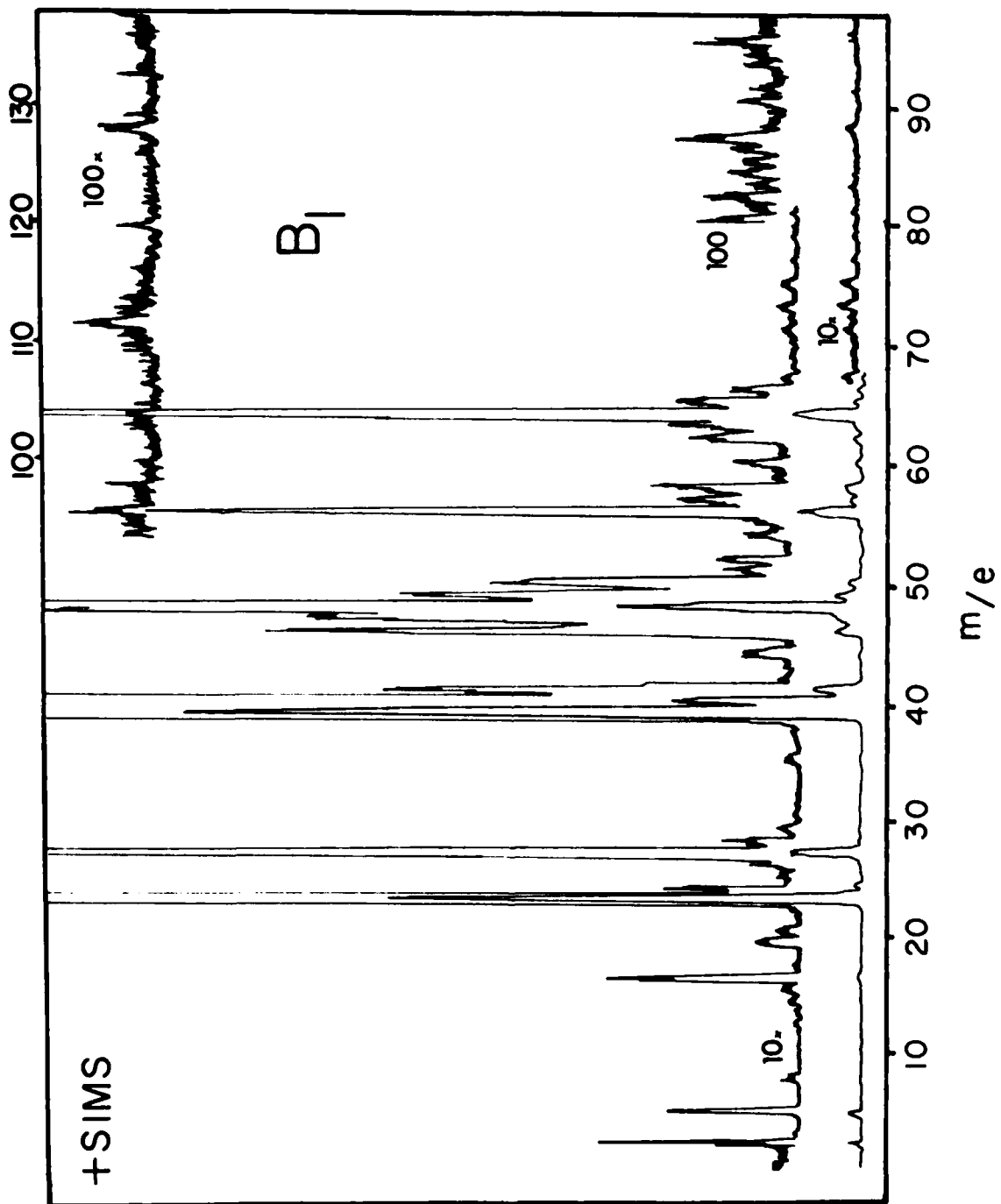


Figure 3. He⁺ SIMS Spectrum of "As Received" Ti-8Al-1Mo-1Sn.

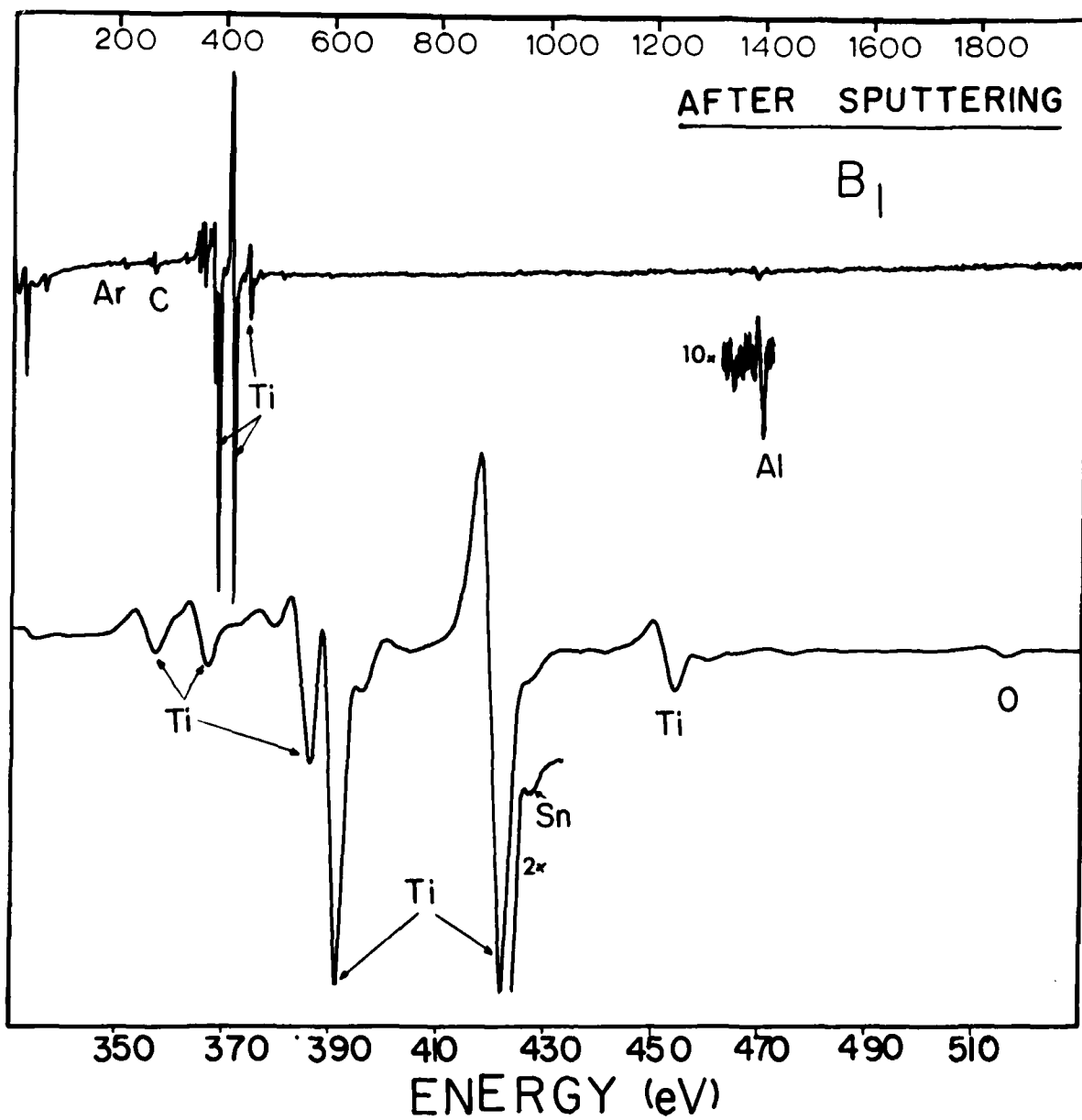


Figure 4. AES Spectra of ES Ti-8Al-1Mo-1Sn.

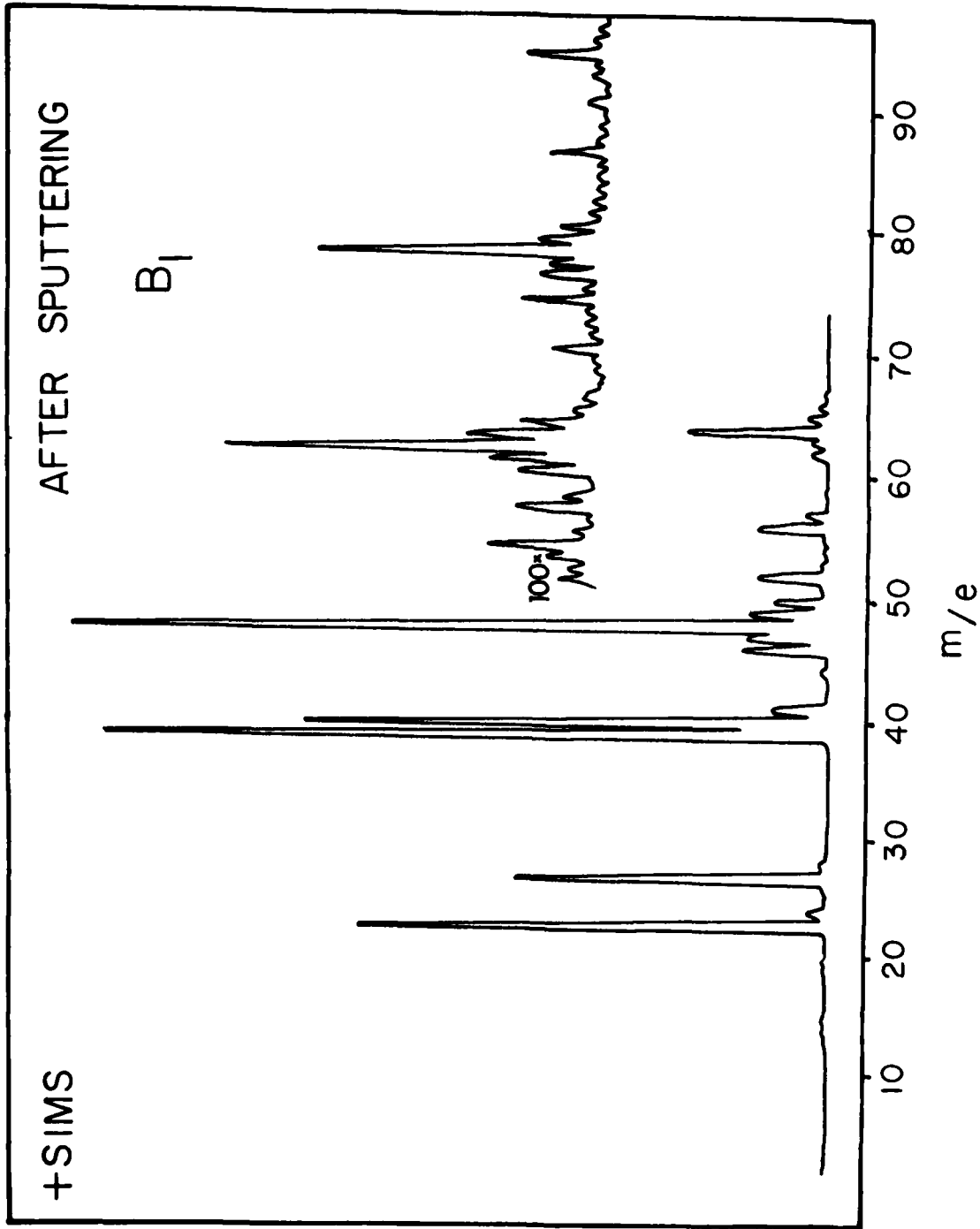


Figure 5. Ar⁺ SIMS Spectrum of ES Ti-8Al-1Mo-1Sn.

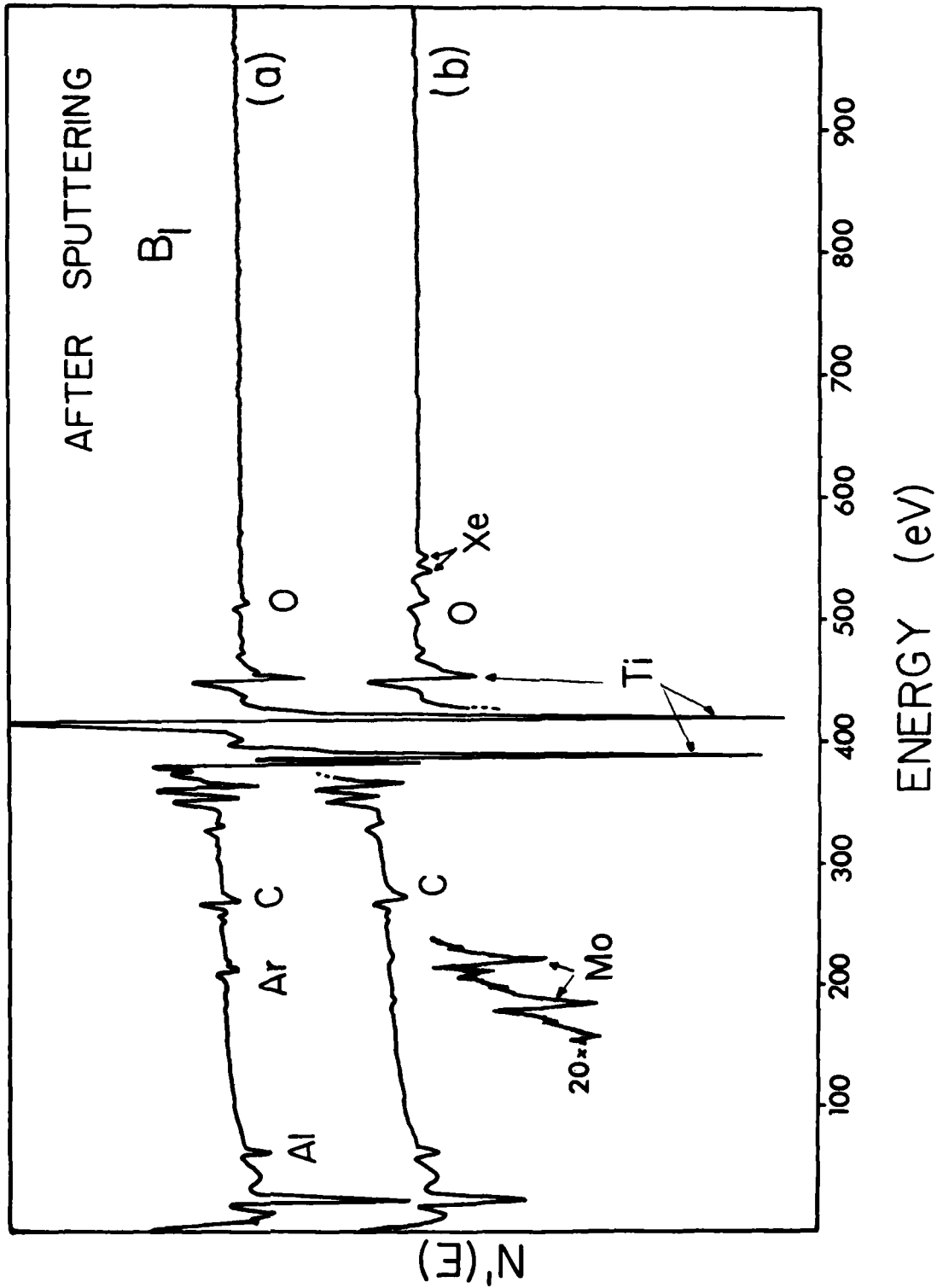


Figure 6. AES Spectra of (a) Argon Sputtered ES and (b) Xenon Sputtered ES Surfaces of Ti-8Al-1Mo-1Sn.

TABLE 2
 AES ELEMENTAL I.D. OF TREATED Ti-8Al-1Mo-1Sn

TREATMENT	ELEMENT IDENTIFICATION										
	Ti (381 eV)	O	C	P	Ca	Na	F	S	Cl	K	Al
1	1	2.3	0.7	x	0.2	x		x	x		x
2	1	2.0	0.6	x	x			x	x		x
3	1	2.3	0.5				x	0.1	x		x
4	1	1.6	0.5	0.1	0.4	0.6	0.7	x	x	x	x
5	1	2.0	0.3	x	x		x	x	x		x
6	1	2.1	0.8	x	x			x	x		x
7	1	2.1	0.5	x	x	x	x	x	x		x
8	1	2.1	0.3		0.2	x		x	x		x

(x APPH RATIO < 0.1)

TABLE 3
SIMS ELEMENTAL I.D. OF TREATED Ti-8Al-1Mo-1Sn

TREATMENT	m/e / positive ion identification														
	16 O	19 F	23 Na	27 Al C ₂ H ₃	35 Cl	39 K	40 Ca	48 Ti	59 AlO ₂ CaF	64 TiO	67 TiF	86 TiF ₂	96 Ti ₂	112 Ti ₂ O	120 Sn
1	x	x	1.9	0.28	x	2.72	0.76	1		0.28			x	x	x
2	x	x	0.8	0.29		0.23	0.29	1	x	0.37			x	x	x
3	x	x	0.9	0.28	x	0.25	x	1		0.22			x	x	
4		0.5	13.0	0.74		0.12	0.73	1	x	x	0.25	x			
5	x	x	1.6	0.14	x	0.23	0.10	1		0.32			x	x	x
6		x	0.2	0.39		x	0.12	1		x			x	x	
7			0.3	0.26		0.10	x	1		x			x		
8			0.4	0.27	x	0.10	0.76	1		x					

(x VALUE < 0.1)

surface sensitive than AES. As shown in Figure 2, Mo was detected on the "as received" surface (spectrum a) but was only present in the first or second monolayer since spectrum b, which was recorded immediately after spectrum a, shows Mo to be nearly depleted by the very gentle He^+ beam.

The Ti_{LMM} Auger peak shapes were nearly identical to TiO_2^1 with some subtle differences observed when fluorine was present. The thickness of the surface oxides as determined by Auger sputter profile analysis and listed in Table 6 ranged from approximately 7.8 nm from treatment 8 to 112 nm for treatment 4. This compares to approximately 14.6 nm for an untreated surface.

Figures 7-10 show the SEM micrographs of the treated surfaces. Some evidence of selective phase etching can be seen in Figures 8 (B_{1-3}), 9 (B_{1-5}), and 10 (B_{1-7}), or treatments 3, 5, and 7, respectively. The fluoro-phosphate treatment, Figure 8 (B_{1-4}) produced the most noticeable topographical change in which the surface oxide has a "sea shell" like appearance.

B. Ti-13V-11Cr-3Al

AES and SIMS spectra from an "as received" surface are shown in Figures 11 and 12, respectively, and the respective ES spectra are shown in Figures 13 and 14. Tables 4 and 5 contain the respective AES and SIMS semiquantitative data obtained from the treated Ti-13V-11Cr surfaces. As with Tables 2 and 3, the values listed in Tables 4 and 5 are normalized to Ti. Both Tables 4 and 5 show the presence of Ti as well as the three alloying elements on all treated surfaces. The surface concentration of the alloying elements in all cases was less than the bulk. The surface of the fluoro-phosphate treated panel contained F but no TiF^+ species was detected by SIMS nor did the Ti_{LMM} peak shape differ from that of TiO_2 . The oxide layers produced on this alloy were all thinner than that of as received panels. The thickest oxide (~ 8 nm) was formed by the sulfo-chromium (6) treatment while the thinnest (~ 2.3 nm) was produced by alkaline (2) treatment. Table 6 lists the oxide thickness resulting from each treatment.

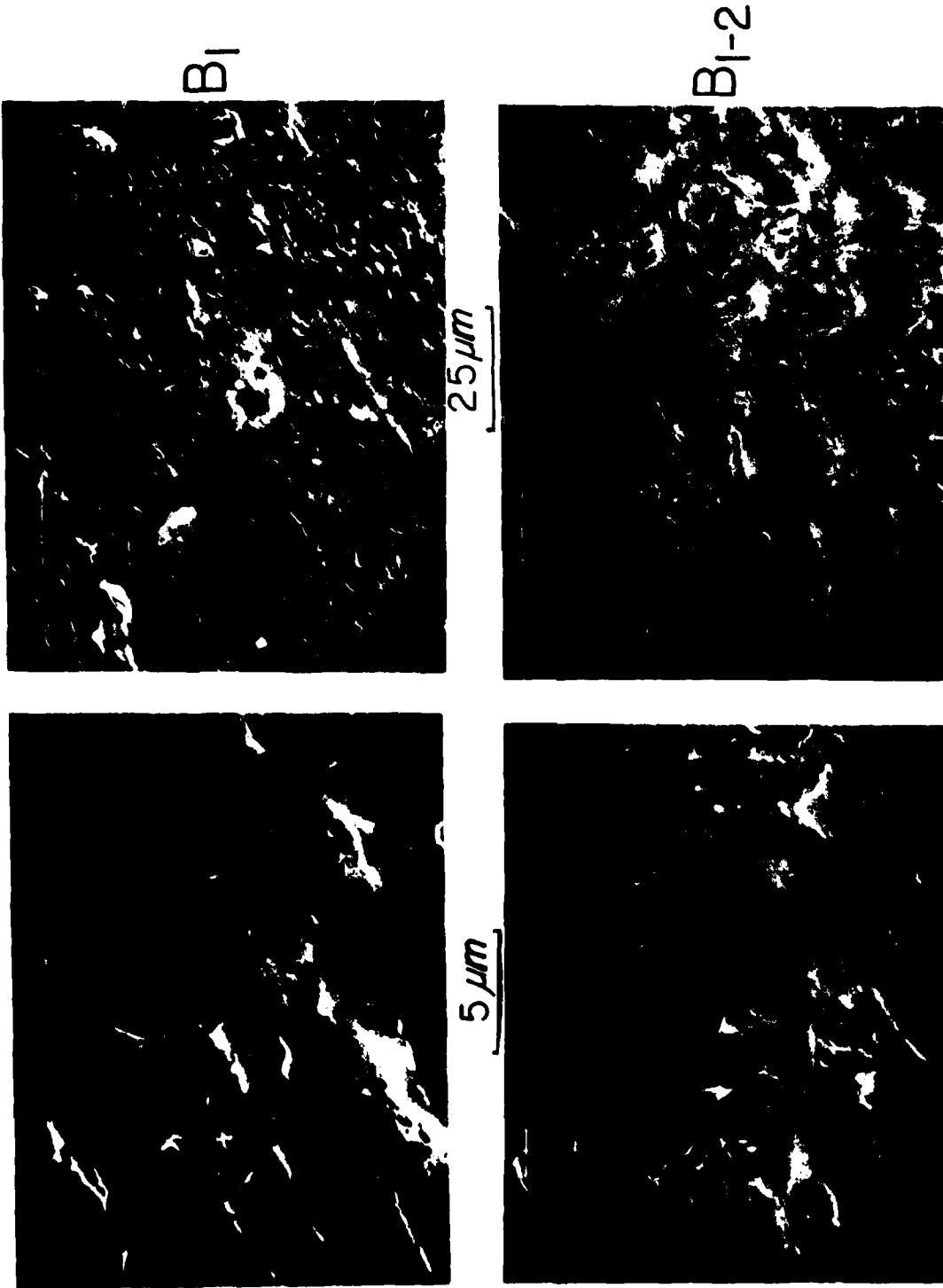


Figure 7. SEM Micrographs of Ti-8Al-1Mo-1Sn Subjected to Treatments 1 (B₁) and 2 (B₁₋₂).

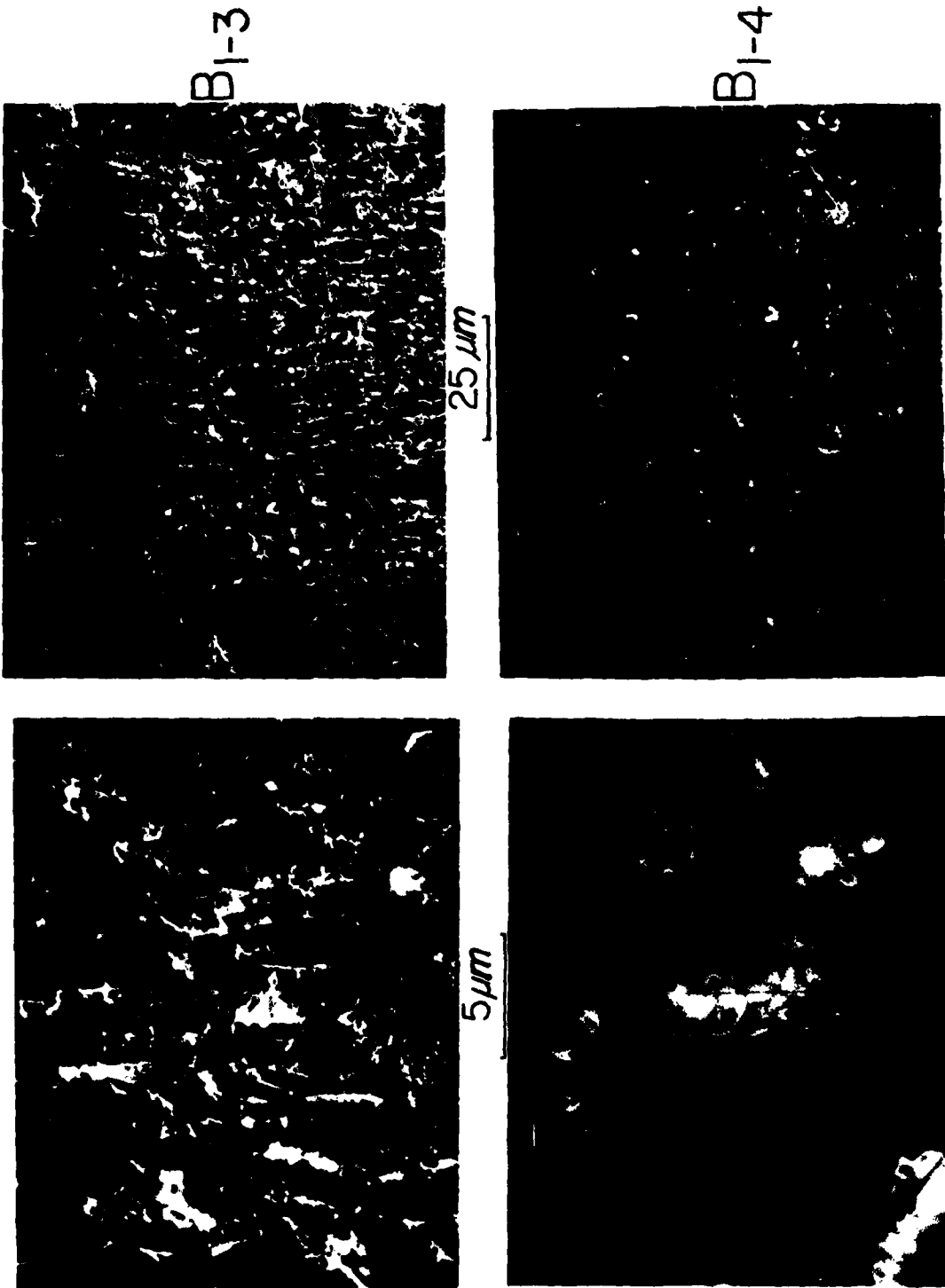
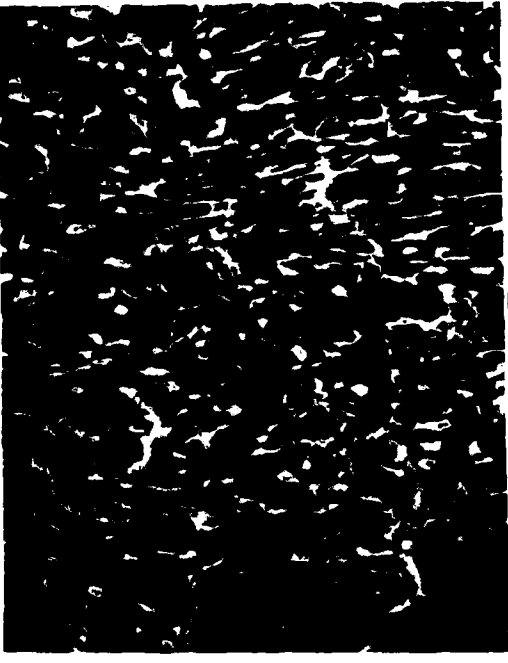


Figure 8. SEM Micrographs of Ti-8Al-1Mo-1Sn Subjected to Treatments 3 (B₁-3) and 4 (B₁-4).

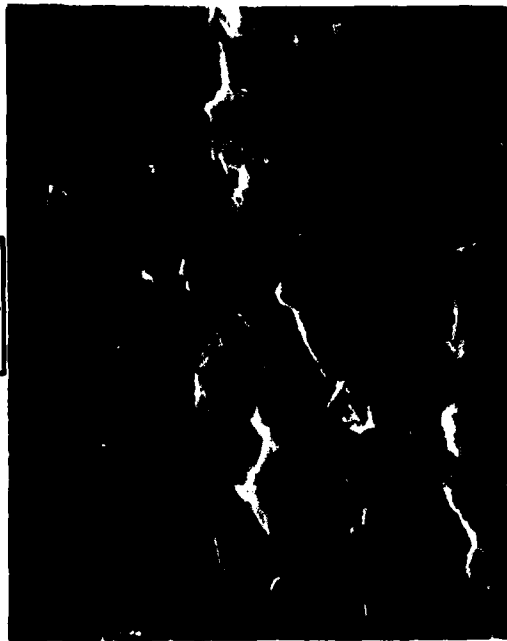


5 μm



25 μm

B1-5



B1-6

Figure 9. SEM Micrographs of Ti-8Al-1Mo-1Sn Subjected to Treatments 5 (B₁₋₅) and 6 (B₁₋₆).

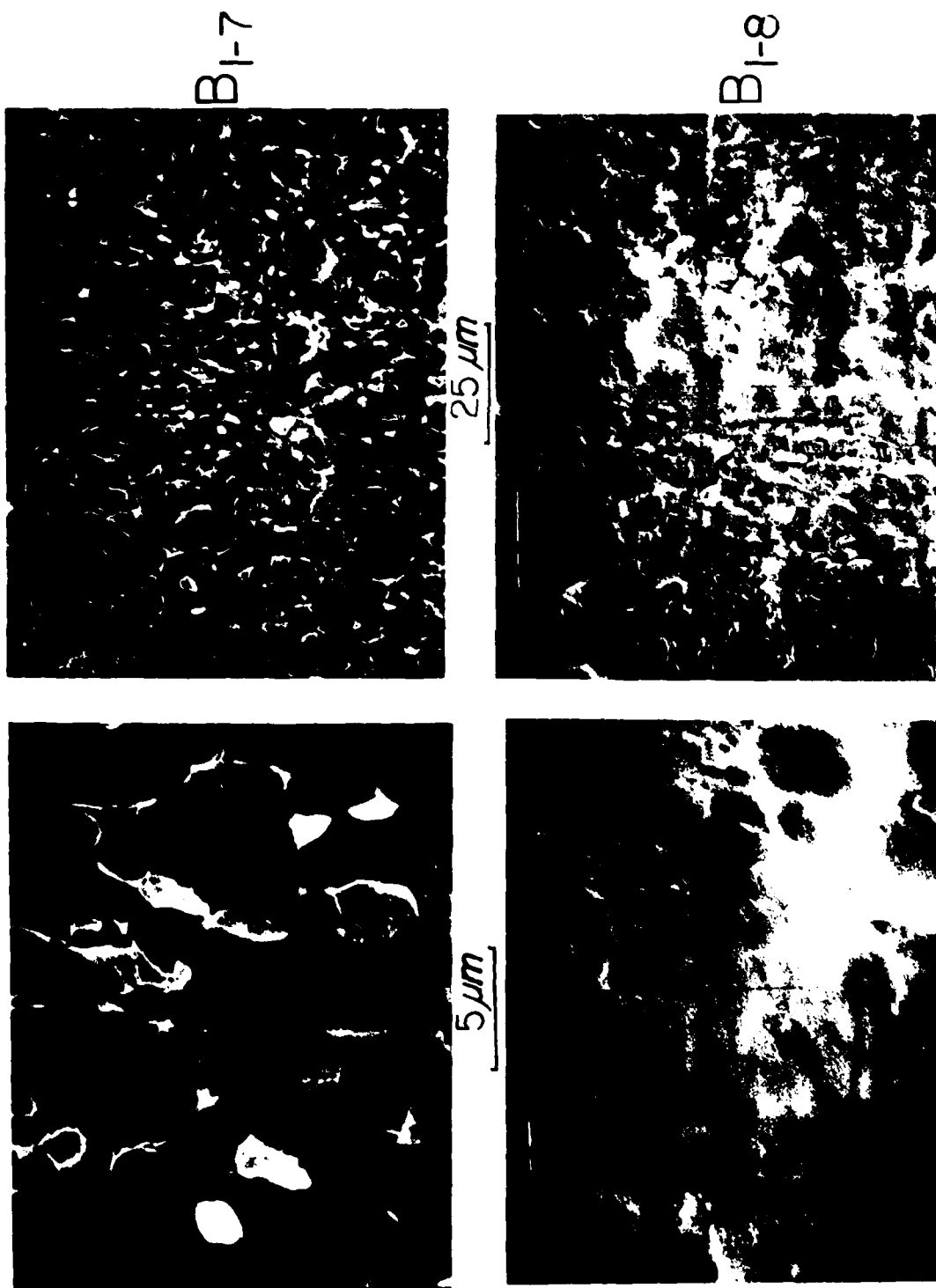


Figure 10. SEM Micrographs of Ti-8Al-1Mo-1Sn Subjected to Treatments 7 (B₁₋₇) and 8 (B₁₋₈).

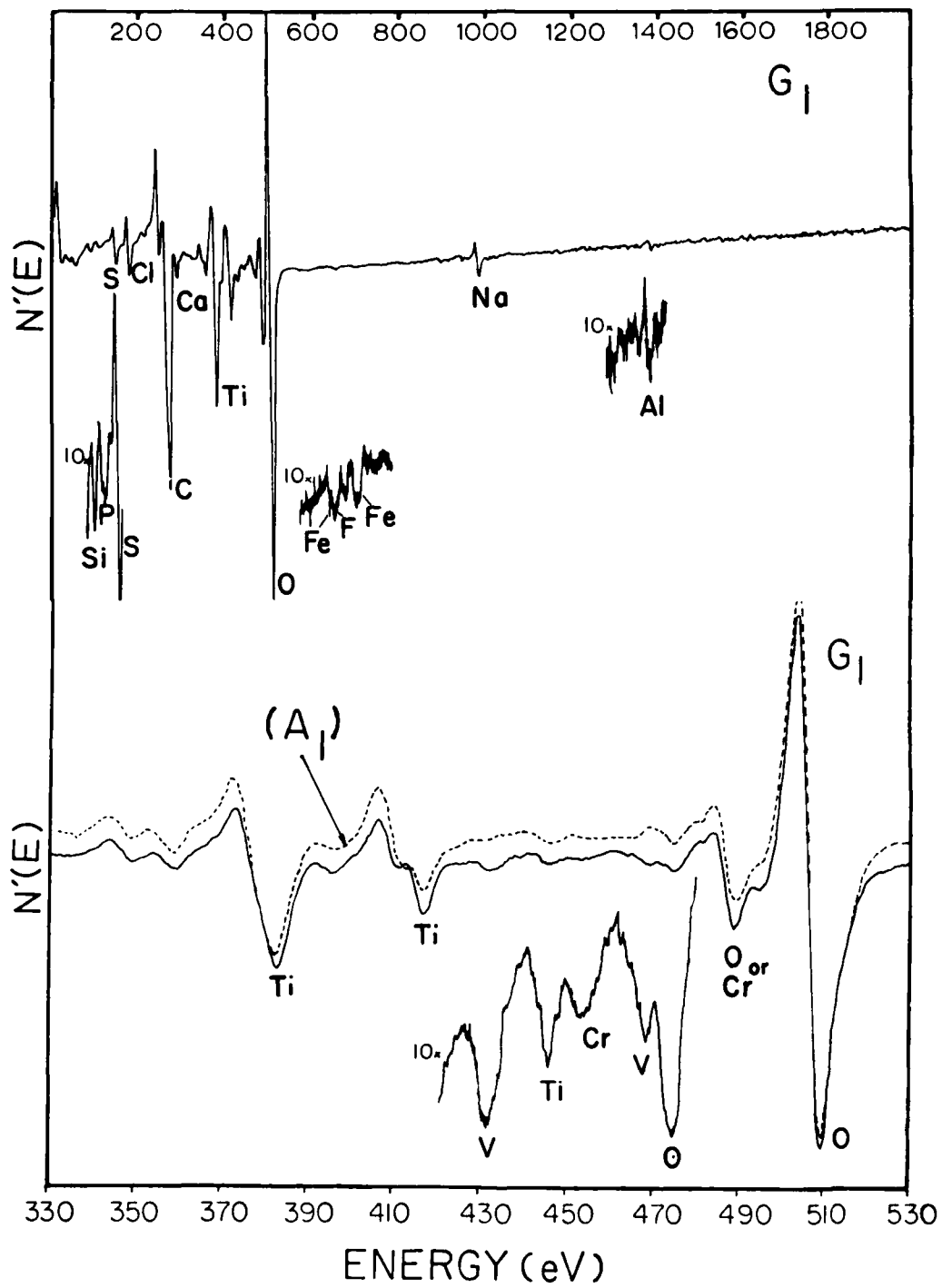


Figure 11. AES Spectra of "As Received" Ti-13V-11Cr-3Al.

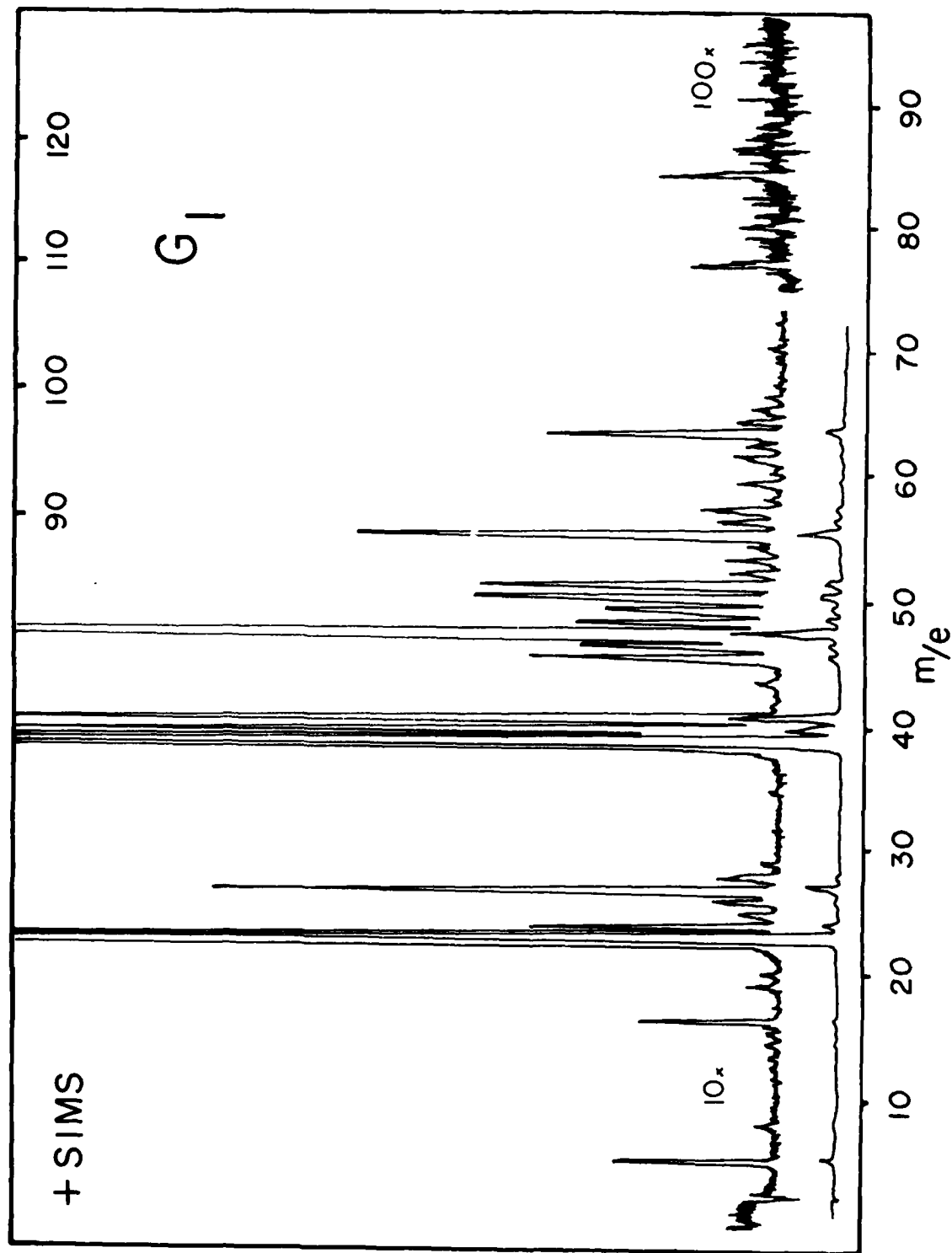


Figure 12. He⁺ SIMS Spectrum of "As Received" Ti-13V-11Cr-3Al.

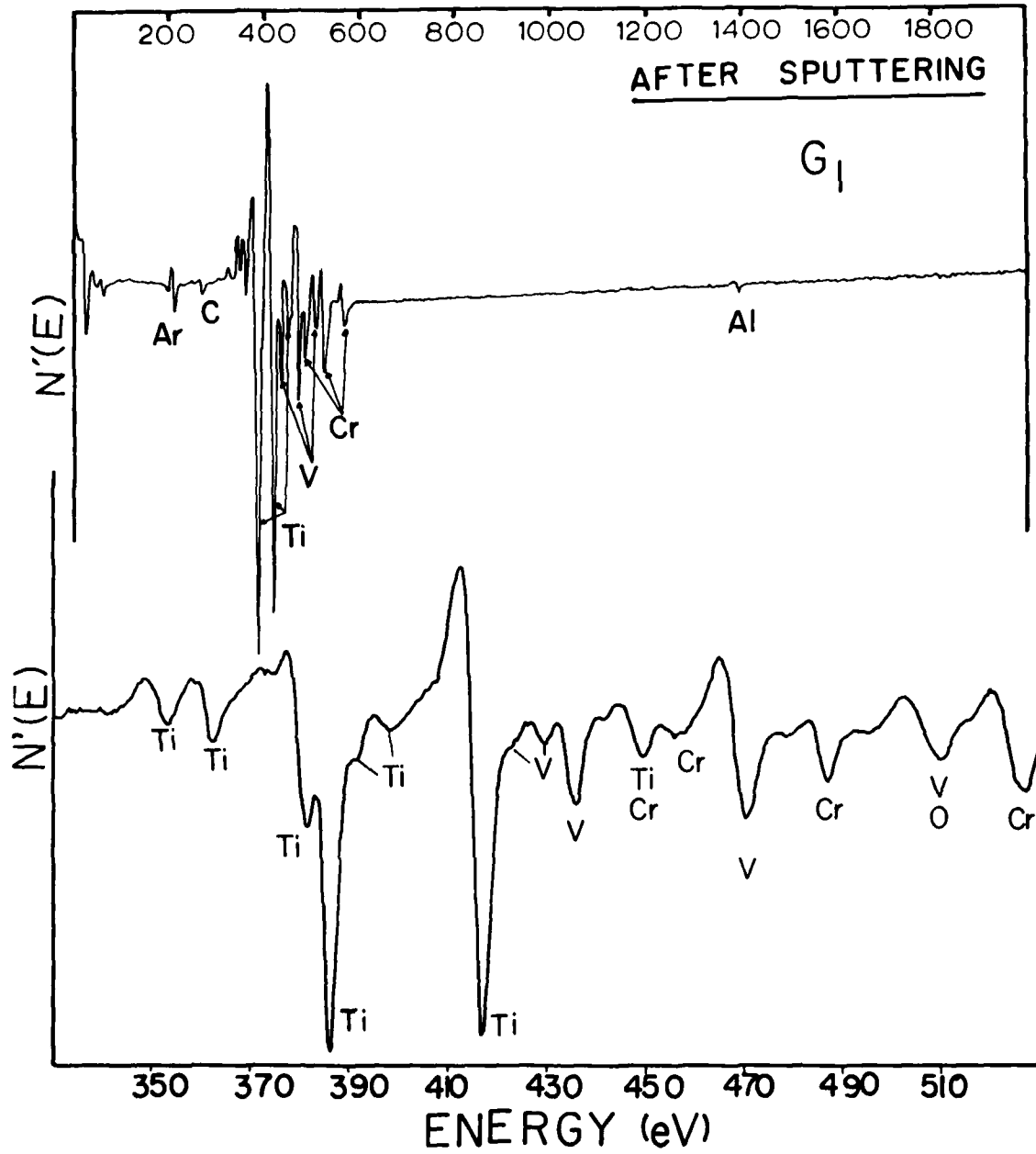


Figure 13. AES Spectra of ES Ti-13V-11Cr-3Al.

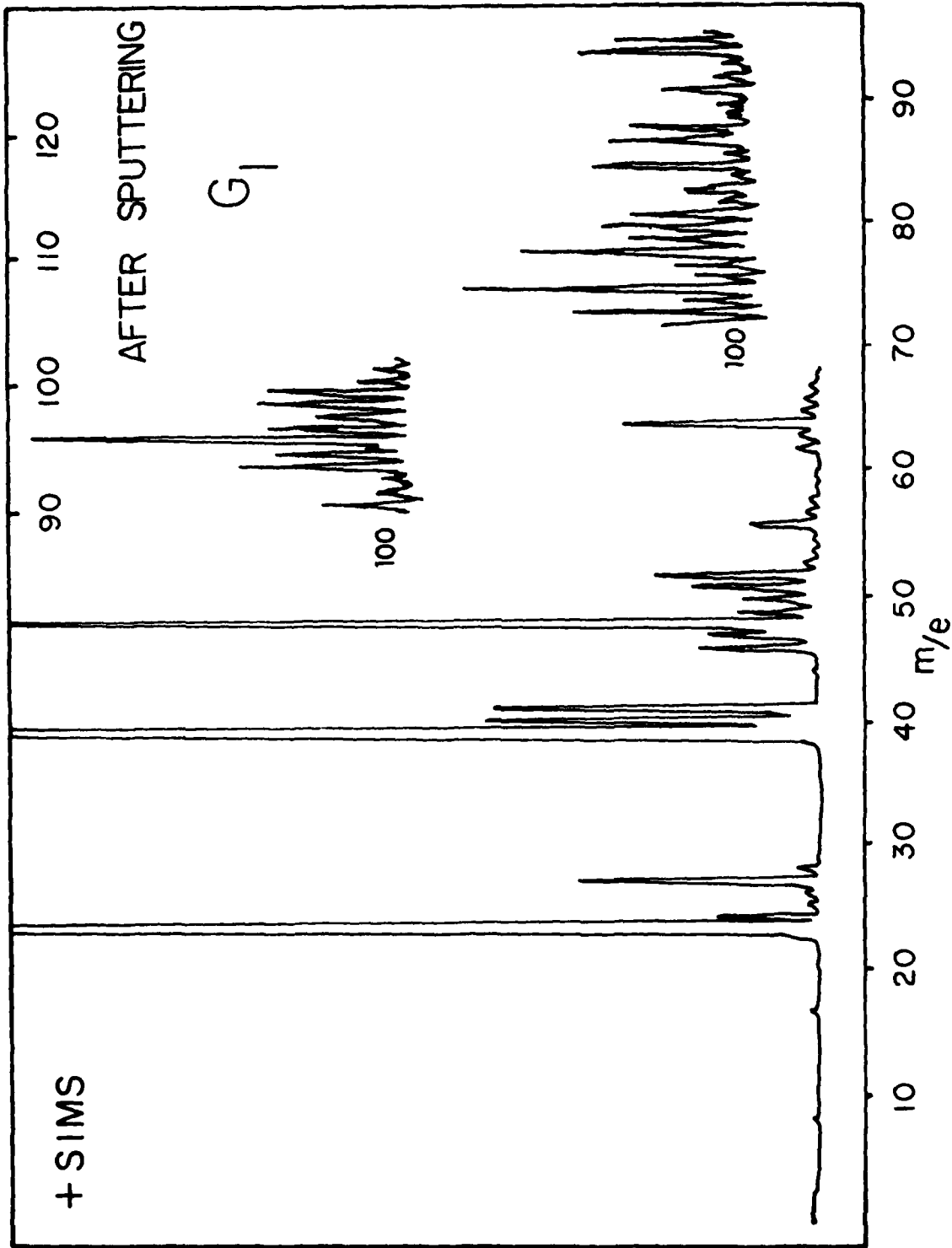


Figure 14. Ar⁺ SIMS Spectrum of ES Ti-13V-11Cr-3Al.

TABLE 4
 AES ELEMENTAL I.D. OF TREATED Ti-13V-11Cr-3Al

TREATMENT	ELEMENT IDENTIFICATION												
	Ti (381 eV)	O	C	P	Ca	Na	F	S	Cl	K	Al	Cr	V
1	1	3.1	1.4	x	0.1	x		0.2	0.3	x	x	x	x
2	1	2.8	1.5	x	0.1	x		x	x		x	x	x
3	1	3.0	1.2		x			x	0.4		x	x	x
4	1	3.1	1.3	x	0.1	x	0.1	x	x		x	x	x
5	1	2.5	0.7					x	x		x	x	x
6	1	2.4	0.8		x	x		x	x		x	x	x
7	1	2.5	0.8		x			0.1	x		x	x	x
8	1	3.5	3.5		0.1	x		x	x		x	x	x

(x APPH RATIO < 0.1)

TABLE 5
SIMS ELEMENTAL I.D. OF TREATED Ti-13V-11Cr-3Al

TREATMENT	m/e / positive ion identification											Al/V	Cr/V		
	16 O	19 F	23 Na	27 C ₂ H ₃ Al	35 Cl	39 K	40 Ca	48 Ti	51 V	52 Cr	64 TiO			67 VO	68 CrO
1	x	x	8.2	0.26	x	>9	0.5	1	0.17	0.13	0.15	x		1.8	1.0
2	x	x	0.8	0.22		0.4	0.6	1	0.12	0.13	0.20	x	x	2.1	1.1
3	x	x	0.7	0.21	x	0.4	0.2	1	0.17	0.19	0.18	x	x	1.4	1.2
4	x	x	>3	0.16	x	0.2	0.5	1	0.18	0.49	0.17	x	x	1.0	2.6
5	x	x	0.3	0.16		x	x	1	0.26	0.16	0.19	x	x	0.6	0.6
6	x	x	0.5	0.13		0.1	0.2	1	0.12	0.24	0.23	x	x	1.1	2.0
7	x	x	0.3	0.15	x	0.1	0.2	1	0.19	0.17	0.19	x	x	0.8	0.9
8	x	x	0.9	0.22	x	0.2	0.8	1	0.13	0.35	0.16	x	x	1.8	2.8

(x VALUE < 0.1)

TABLE 6
OXIDE THICKNESS IN NANOMETERS DETERMINED BY
AUGER SPUTTER PROFILE ANALYSIS FROM TREATED
Ti-8Al-1Mo-1Sn AND Ti-13V-11Cr-3Al

Treatment	Ti-8Al-1Mo-1Sn	Ti-13V-11Cr-3Al
1	14.6	9.6
2	15.7	2.3
3	17.8	6.5
4	111.8	6.8
5	17.8	2.3
6	12.2	7.9
7	13.3	4.0
8	7.8	5.7

Figures 15-18 contain the SEM micrographs from the eight treated surfaces.

IV. DISCUSSION

The advantage and necessity of using several surface analytical techniques was very evident in this work. For example, the Ti_{LMM} Auger peaks at 418 and 451 eV as well as oxygen at 510 eV and its lower energy plasmons between 450 and 500 eV overlap the major Sn, Cr, and V peaks between 400 and 530 eV, making it difficult to analyze for small amounts of these elements in the presence of Ti and O. Although Cr and V are shown as being detected by AES in Table 2, absolute certainty of their presence was provided by SIMS, since no overlapping problems occur for these elements in this technique.

The detection of Sn by AES is further complicated when Sn is oxidized. Normally, the major Sn_{MNN} peak positions are 430 and 437 eV. However, when Sn is oxidized, the peaks shift to a lower energy by 5-6 eV². This shift is toward the Ti_{LMM} peaks and, therefore, small amounts of Sn do not adequately change AES spectral features, as in the case of V. In this case, SIMS or ISS can be used to detect the presence of Sn.

Neither AES nor SIMS could verify the presence of Mo on any of the treated specimens. ISS data shows that Mo is present within the first few monolayers and is quickly removed by sputtering. The detection of low concentrations of Mo, especially when oxidized or in the presence of Cl is very difficult. The AES Cl peak at 181 eV interferes with the 186 eV Mo peak and the Mo 221 eV peak decreases in intensity with respect to the 186 eV peak when Mo is oxidized.³ In order to detect the low concentration of Mo in the bulk an ES surface had to be established with Xe, rather than Ar sputtering, because of Ar peak interferences with Mo peaks at 186 and 221 eV.

Unlike AES, SIMS is capable of detecting molecular species such as those reported in Tables 3 and 5. One of the problems

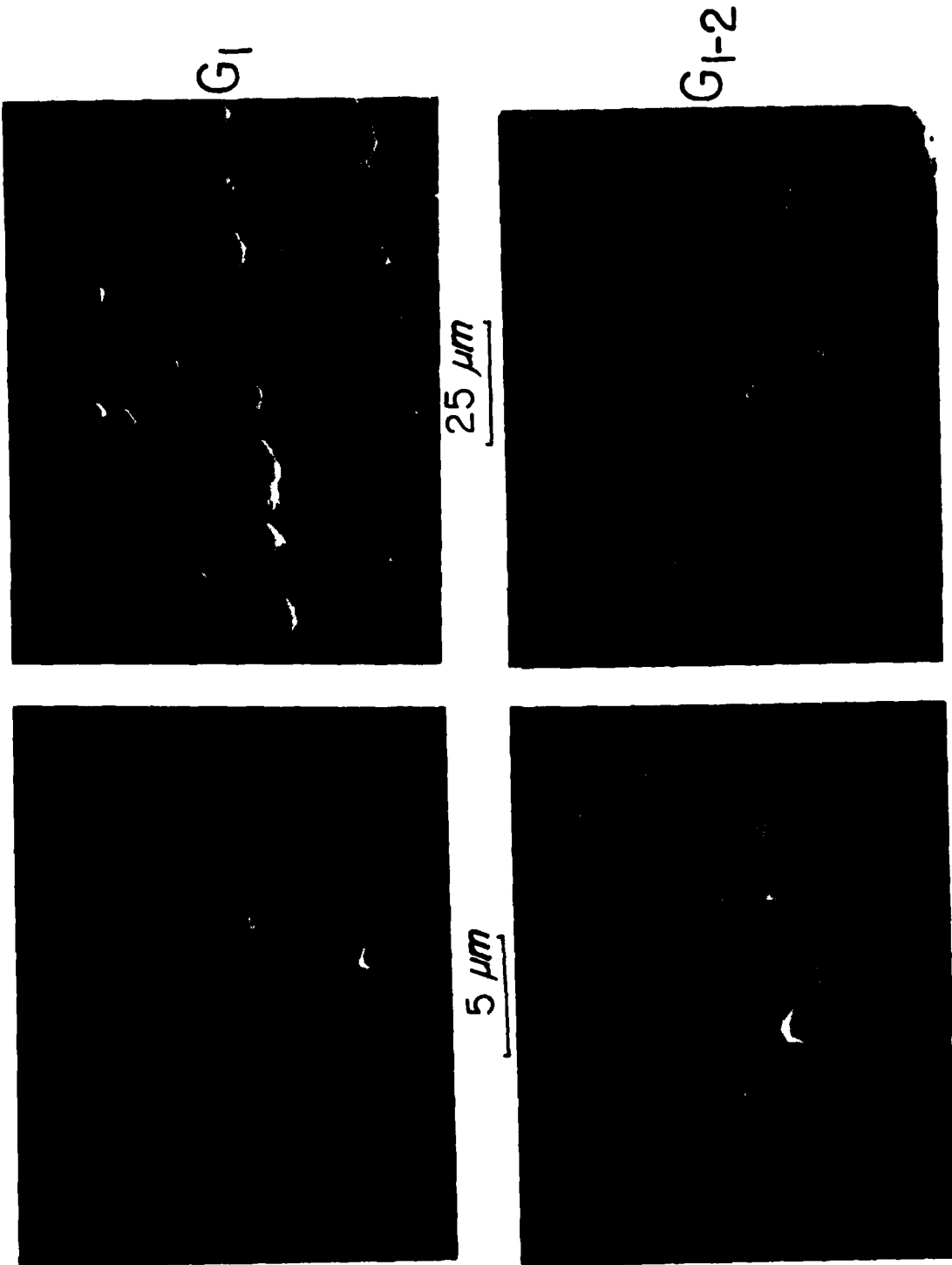


Figure 15. SEM Micrographs of Ti-13V-11Cr-3Al Subjected to Treatments 1 (G_1) and 2 (G_1-2).

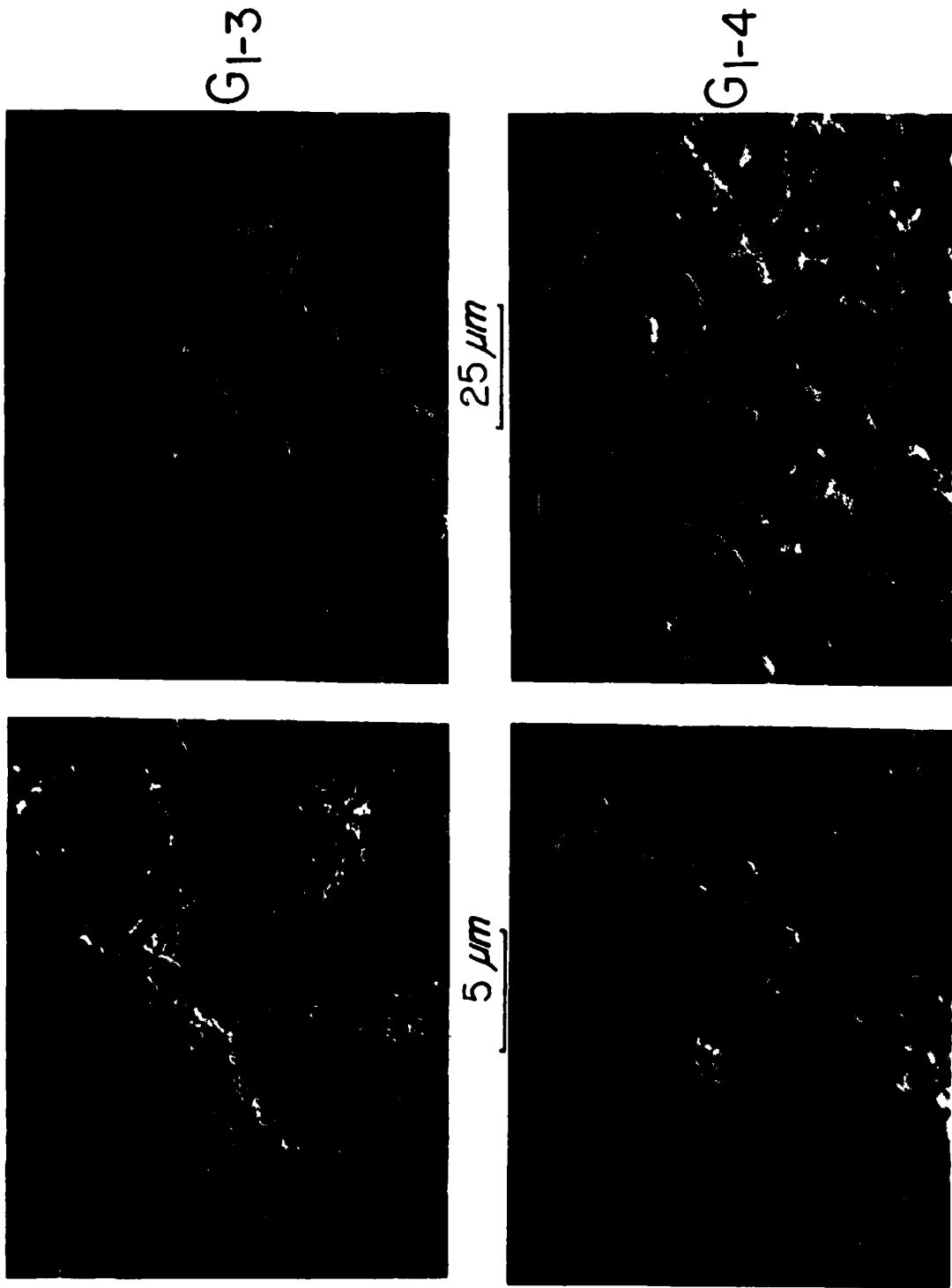


Figure 16. SEM Micrographs of Ti-13V-11Cr-3Al Subjected to Treatments 3 (G₁₋₃) and 4 (G₁₋₄).

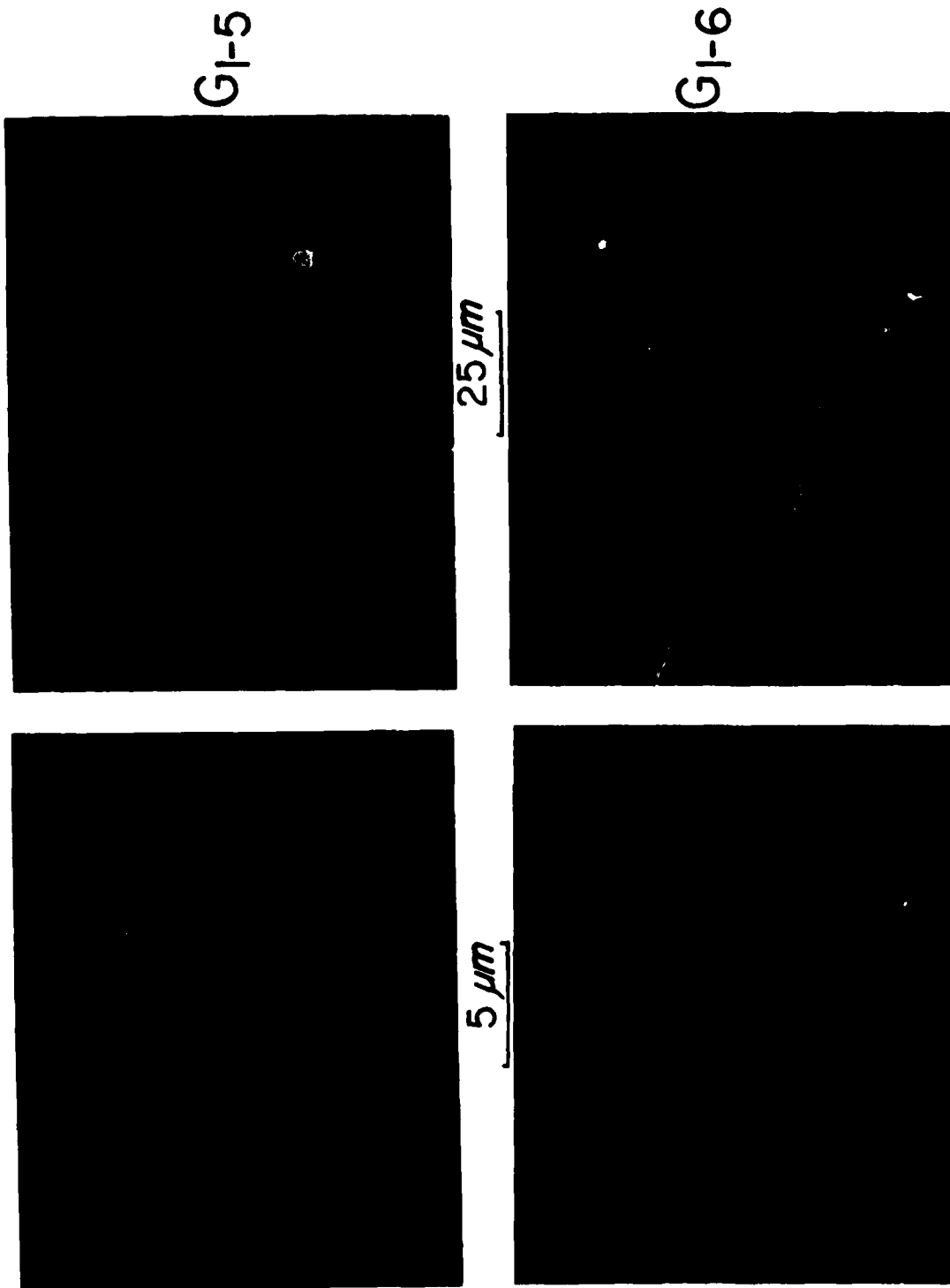


Figure 17. SEM Micrographs of Ti-13V-11Cr-3Al Subjected to Treatments 5 (G₁₋₅) and 6 (G₁₋₆).

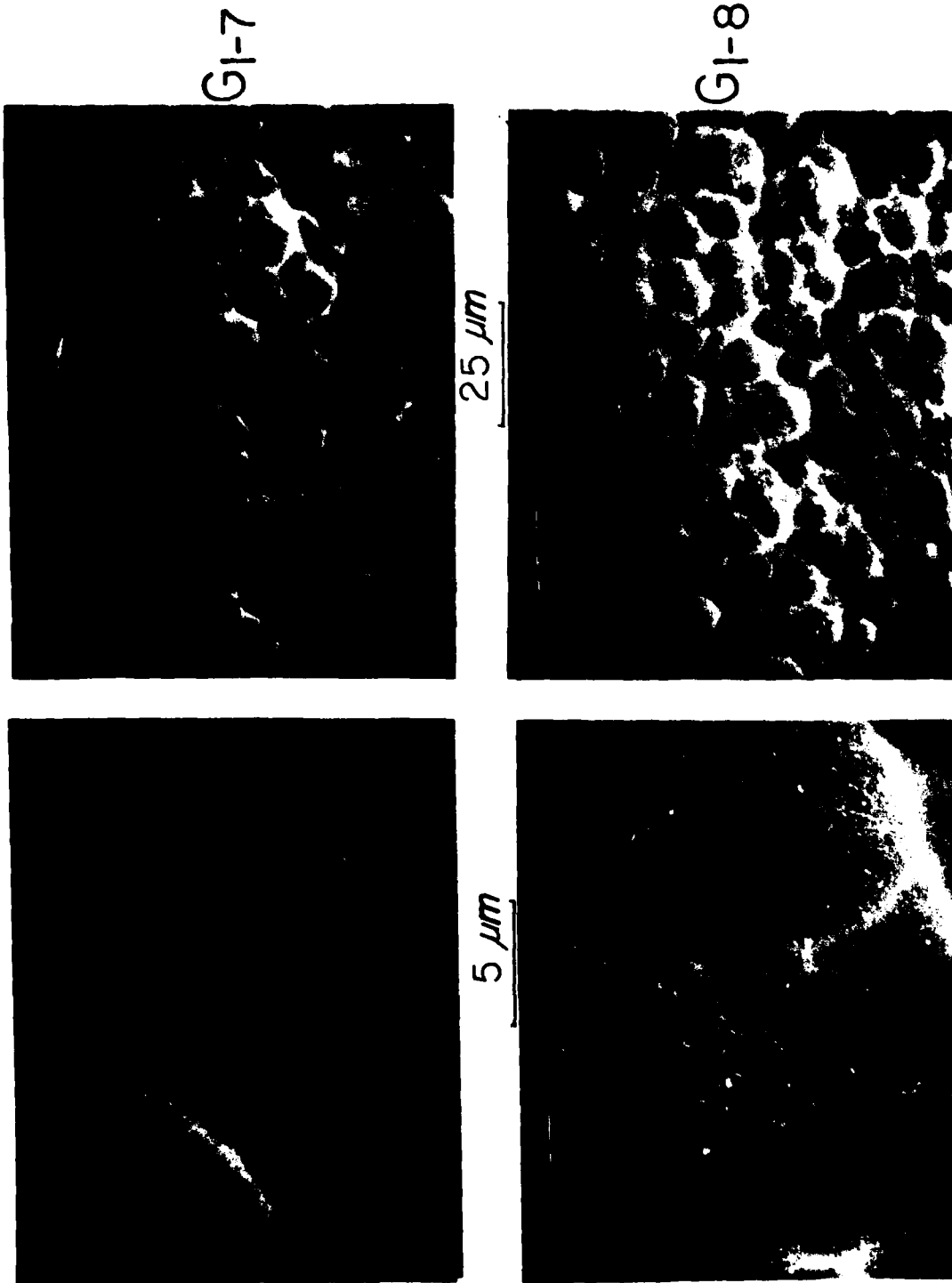


Figure 18. SEM Micrographs of Ti-13V-11Cr-3Al Subjected to Treatments 7 (G₁₋₇) and 8 (G₁₋₈).

with reporting molecular species is knowing for sure the origin of the species. For example, it is difficult to determine whether a particular species was present on a surface or created during sputtering. Such is the case with TiO^+ , $TiOF^+$, and TiF^+ detected on Ti-8Al-1Mo-1Sn subjected to the fluoro-phosphate (4) treatment (Figure 19). In this case, the limited ability of AES to detect chemical state differences was used to determine if the bonding state of Ti was different on this specimen versus one in which fluorine was not detected. As shown in Figure 20, the Ti_{LMM} peaks from this surface had subtle differences in their shapes compared to nonfluoride containing surfaces (Figure 17) and standard TiO_2 . This is an indication that Ti was in a slightly different bonding state than in TiO_2 . Perhaps it is bound to both O and F as an oxyfluoride.

In the case of Ti-13V-11Cr-3Al no $Ti-F^+$ species was observed in the SIMS data shown in Figure 21 and the Ti_{LMM} Auger peak shapes in Figure 22 were identical to TiO_2 . The Ti_{LMM} peak shapes from the other treated surfaces were also identical to TiO_2 .

The SEM was extremely valuable, not only for the characterization of surface topography, but in determining oxide film thicknesses in order to establish sputter rates for Auger sputter profile analysis.

V. CONCLUSIONS

Based on the characterization data presented, the following conclusions are made about the effects of the chemical treatments listed in Table 1 on Ti-8Al-1Mo-1Sn and Ti-13V-11Cr-3Al.

1. No single surface analytical technique can thoroughly characterize Ti alloy surfaces for their elemental, chemical, and physical properties.
2. The effects of a particular chemical treatment may not be the same for each alloy.

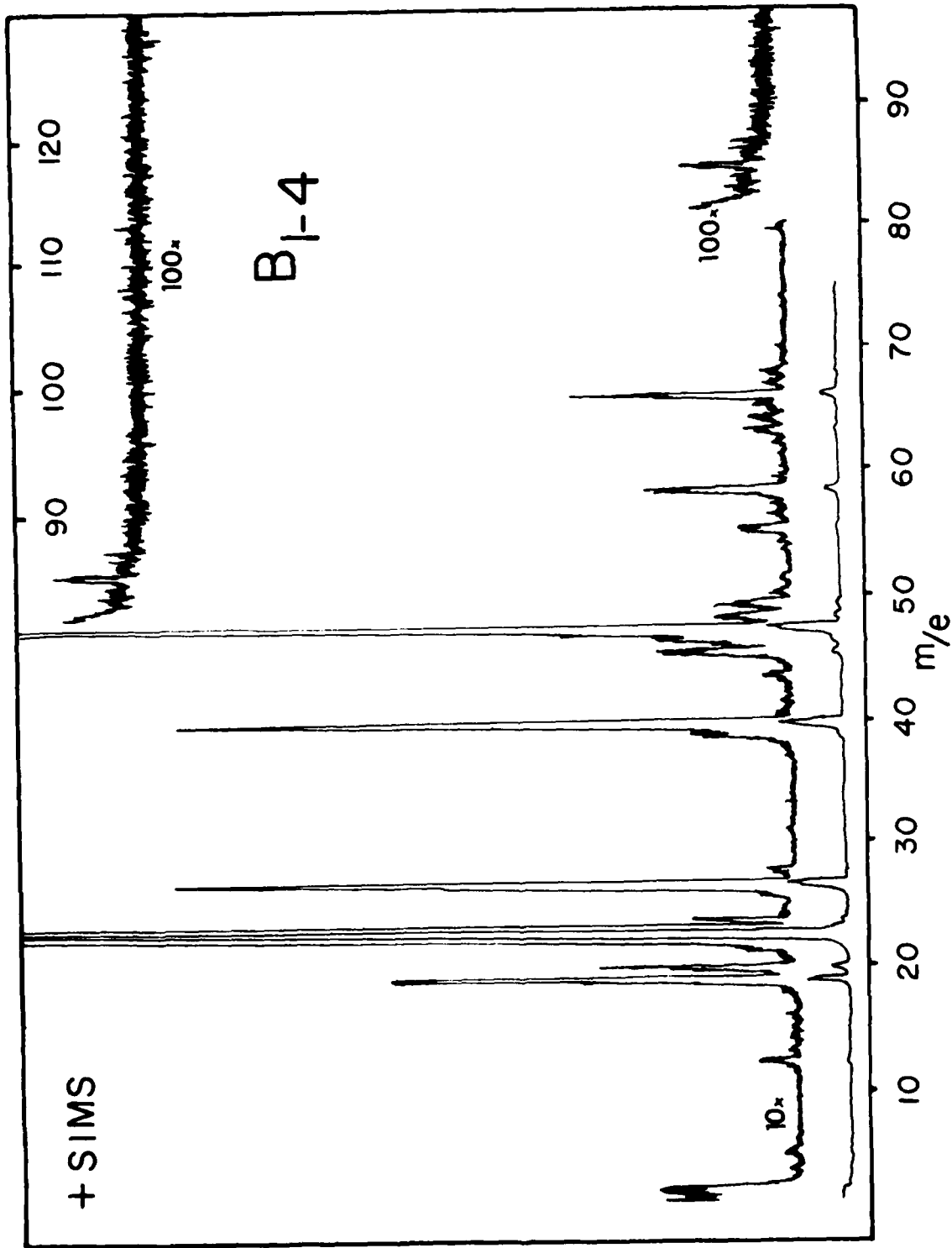


Figure 19. He^+ SIMS Spectrum of Ti-8Al-1Mo-1Sn Subjected to Treatment 4.

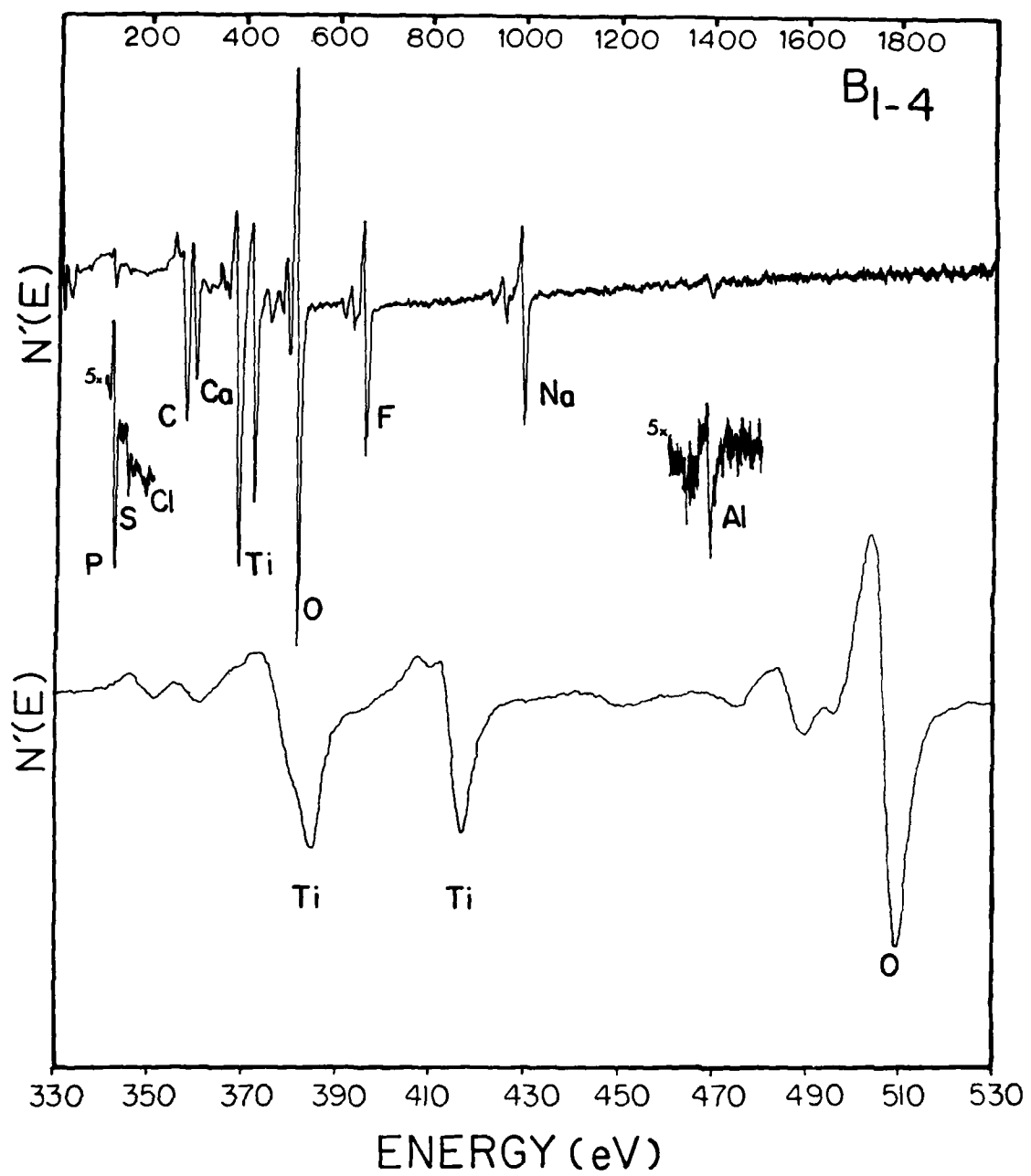


Figure 20. AES Spectra of Ti-8Al-1Mo-1Sn Subjected to Treatment 4

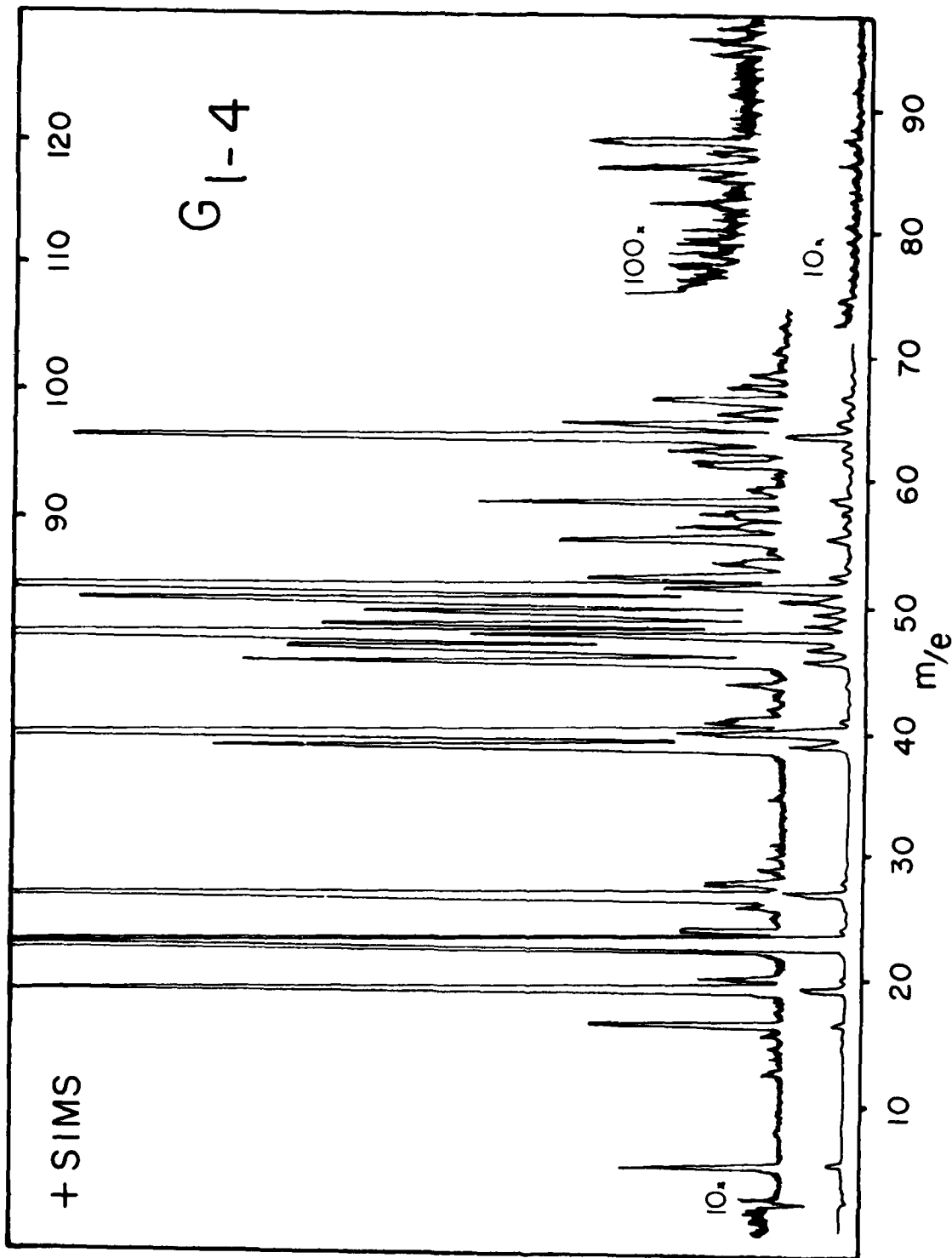


Figure 21. He^+ SIMS Spectrum of Ti-13V-11Cr-3Al Subjected to Treatment 4.

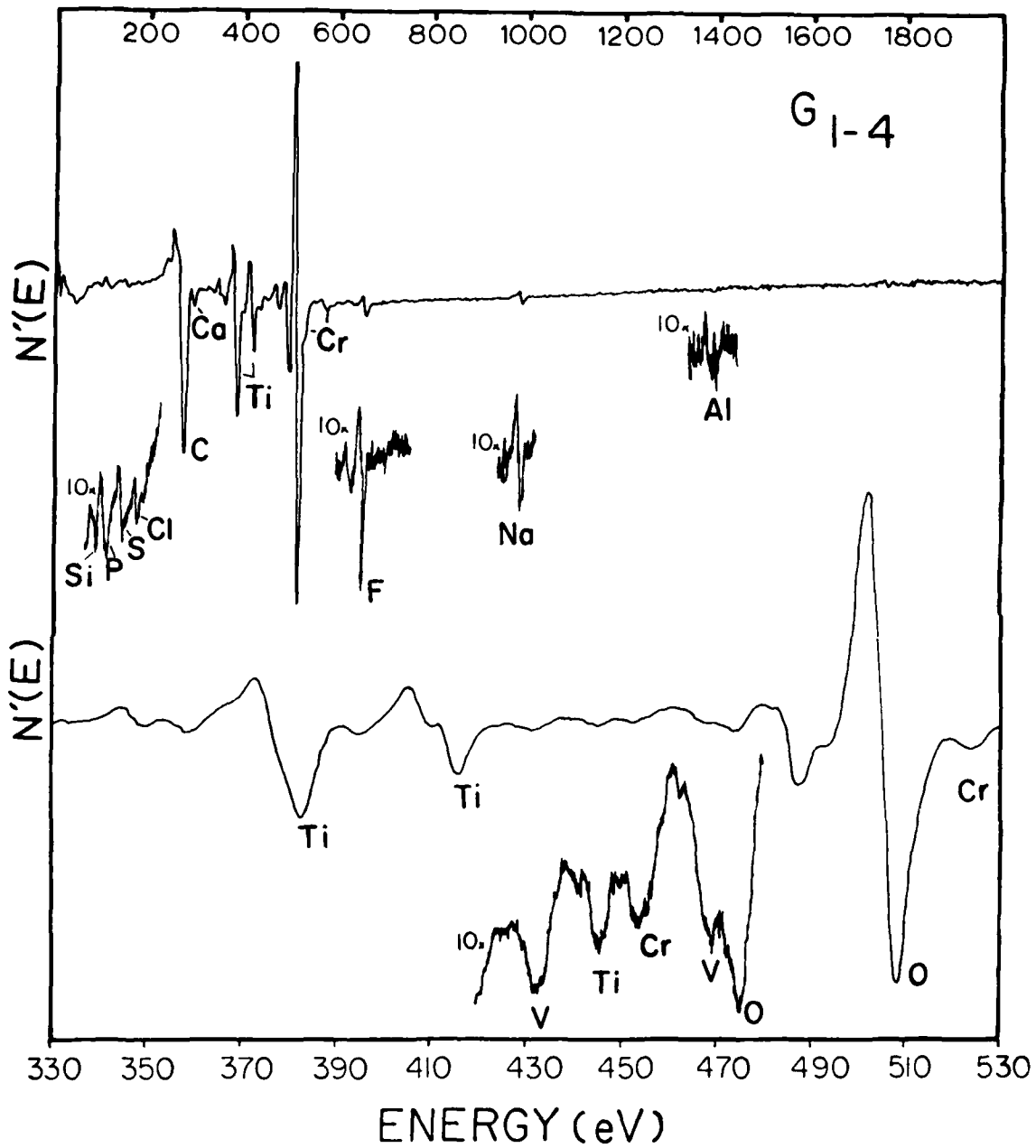


Figure 22. AES Spectra of Ti-13V-11Cr-3Al Subjected to Treatment 4.

3. Chemical treatments 2 through 8 replace the original oxide with a new one containing traces of elemental species common to a particular treatment.

4. The α Ti-8Al-1Mo-1Sn is etched at a faster rate than β by treatments 3, 5, and 7.

5. The oxide produced on Ti-8Al-1Mo-1Sn by the fluorophosphate treatment is not TiO_2 but one in which Ti may be chemically bound as an oxyfluoride.

REFERENCES

1. J. S. Solomon and W. L. Baun, *Surface Science*, 51, 228 (1975).
2. R. A. Powell, *Applications of Surface Science*, 2, 397 (1979).
3. M. P. Nooker, J. T. Grant, and T. W. Haas, *J. Vac. Sci. Technol.*, 12, 325 (1974).